Energy Nexus 23 (2026) 100742

Contents lists available at ScienceDirect

Energy Nexus

journal homepage: www.elsevier.com/locate/nexus

Full Length Article

Techno-energy-economic feasibility assessment of hybrid, deep geothermal plants for sustainable, reliable power generation in cold environments

Alireza Dehghani-Sanij [a,b,*], Mohammad Hadi Ghasemi [c], Andrew Wigston [b], Kushsairy Kadir [d,**], Maurice B. Dusseault [a,e], Grant D. Wach [f]

[a] Department of Mechanical and Mechatronics Engineering, University of Waterloo, Waterloo, ON N2L 3G1, Canada
[b] CanmetENERGY–Ottawa, Natural Resources Canada (NRCan), Ottawa, ON K1A 1M1, Canada
[c] Malaysia France Institute, Universiti Kuala Lumpur (UniKL MFI), 43650, Selangor, Malaysia
[d] British Malaysian Institute, Universiti Kuala Lumpur (UniKL BMI), 53100, Selangor, Malaysia
[e] Department of Earth and Environmental Sciences, University of Waterloo, Waterloo, ON N2L 3G1, Canada
[f] Department of Earth and Environmental Sciences, Dalhousie University, Halifax, NS B3H 4R2, Canada

ARTICLE INFO

Keywords:
Geothermal plant
Hybrid system
Levelized cost of electricity
Renewable
Sustainable development

ABSTRACT

Due to increasing global energy demand and environmental concerns, reliable, sustainable, and renewable energy systems are increasingly needed, particularly for remote cold-region communities dependent on fossil-fuel-based electricity generation. This research presents a techno-energy-economic feasibility assessment of a hybrid, deep geothermal plant (HDGP) integrating a single-stage binary-cycle geothermal system with wind turbines, photovoltaic panels, battery storage medium, and a backup diesel generator to provide reliable baseload electrical power in cold environments. Fort Liard, located in Canada's Northwest Territories, is selected as the case study due to its favourable geothermal potential but with a heavy dependence on diesel-based electricity generation. The research introduces an innovative HOMER™-based geothermal modelling approach in which geofluid is treated as an equivalent fuel source for system optimization and long-term performance evaluation. Actual climate and geological information, operational data, market-based costs, and load profiles are utilized for the techno-energy-economic analysis. The results indicate that the optimized HDGP can sustainably supply the community's electrical demand for 30+ years while reducing geothermal operating intensity through renewable load sharing. The optimal wind and solar capacities provide ~50% of the annual electricity demand, extending the estimated geothermal operational lifecycle from 30 to ~43 years. The levelized cost of electricity for the HDGP is estimated at ~0.27 CAD$/kWh, ~2.6 times lower than the existing diesel-based electricity cost of ~0.70 CAD$/kWh. The economic analysis illustrates an internal rate of return of ~10.7% and a payback duration of ~13 years. This feasibility assessment can be applied to other cold environments worldwide with similar geological and social attributes. The research also aligns with the UN Sustainable Development Goals, adopted in 2015, defined to reach the world's 2030 climate targets.

1. Introduction

Energy is a crucial and integral factor in supporting well-being and driving the social, technological, economic, industrial, and sustainable development of societies worldwide [1], and guided by the UN Sustainable Development Goals (SDGs). Its demand and utilization are growing dramatically for various reasons, the primary ones being the explosion in the world's population [2] and the concurrent escalation in urbanization and industrialization [3,4]. Historically, carbon-based, non-renewable (CBNR) energy sources—such as wood and forestry residues (early) and oil, coal, and natural gas (later)—have governed the global energy market [5]. It is reported that CBNR energy sources and nuclear currently account for ~60% and ~10% of global electrical power production, respectively, whereas renewables are responsible for ~30% [6]. However, reliance on CBNR energy sources has led to energy crises, resource scarcity, environmental issues—such as global warming, climate change, and ecosystem degradation—as well as significant health risks.

To lessen the environmental footprint—particularly addressing

* Corresponding author at: Department of Mechanical and Mechatronics Engineering, University of Waterloo, Waterloo, ON N2L 3G1, Canada.
** Corresponding author.
E-mail addresses: a7dehgha@uwaterloo.ca (A. Dehghani-Sanij), kushsairy@unikl.edu.my (K. Kadir).

https://doi.org/10.1016/j.nexus.2026.100742

Available online 13 June 2026

Nomenclature

CRF	Capital recovery factor
$C_{ann,tot}$	Total annualized cost CAD$/yr
$C_{P,gf}$	Specific heat capacity of geo-fluid kJ/kg· °C
C_{rep}	Replacement cost CAD$
C_t	Annual cost in year *t* CAD$
C_0	Initial investment CAD$
E_{served}	Annual electrical energy served kWh/yr
f	Nominal inflation rate %
i	Nominal discount rate %
i_{real}	Real discount rate %
LHV_{gf}	Lower heating value of brine-fuel MJ/kg
$\dot{m}_{gf}$	Mass flow rate of geo-fluid kg/s
R_{comp}	Component lifetime Hours
R_{proj}	Project lifetime Hours
R_{rem}	Remaining lifetime Hours
R_{rep}	Replacement cost duration Hours
SOC_{min}	Minimum state of charge %
ρ_{gf}	Geo-fluid (brine) density kg/m^3
ΔT_{gf}	Geo-fluid temperature difference across the heat exchanger °C

Abbreviati

BSSs	Battery Storage Systems
CBNR	Carbon-Based, Non-Renewable
CNT	Canada's Northwest Territories
COMFAR	Computer Model for Feasibility Analysis and Reporting
CRF	Capital Recovery Factor
CSP	Concentrated Solar Power
DOD	Depth of Discharge
FL	Fort Liard
GBHSs	Geothermal-Based Hybrid Systems
GE	Geothermal Energy
HDGP	Hybrid Deep Geothermal Plant
HOMER	Hybrid Optimization of Multiple Energy Resources
HRES	Hybrid Renewable Energy System
HRPG	Hybrid Renewable Power Generation
IRR	Internal Rate of Return
LCOE	Levelized Cost of Electricity
NPC	Net Present Cost
NPV	Net Present Value
ORC	Organic Rankine Cycle
O&M	Operation and Maintenance
PD	Payback Duration
PV	Photovoltaic
SDGs	Sustainable Development Goals
SOC	State of Charge
UPS	Uninterruptible Power Supply

concerns related to the release of greenhouse gases into the atmosphere—while meeting the world's energy demands, ensuring energy security, and reaching sustainable development and decarbonization objectives, a pressing transition to clean, sustainable, and reliable energy sources is needed [7,8]. Among these, geothermal energy (GE)—whether utilized individually or in hybrid configurations with other energy sources and storage methods—offers a viable, environmentally friendly, and reliable solution to achieve the objectives mentioned above by delivering clean, dispatchable, stable, and baseload energy (heat and electrical power) necessities for societies [9]—especially those located in remote, isolated jurisdictions and islands with suitable geothermal resources [10,11]. It is reported that by early 2025, geothermal-based power plant technologies generated nearly 16.8 GWe across 35 countries [12], with projections estimating an increase to around 160 GWe by 2050 [13].

Even though GE presents several benefits—including local availability, almost zero-to-low CO_2 emissions, climate independence, and baseload capability with minimal influence from geopolitics or fluctuations in energy demand [14,15]—it still encounters various issues. The primary issue is the decline in thermal energy transfer rates from geo-reservoirs over time if not appropriately managed, leading to reduced productivity [16]. The rate of loss depends on the amount of thermal energy extracted and the temperature of the re-injected fluid, both influenced by the system's production rate and the reservoir's thermal energy capacity and characteristics. This research addresses this issue by designing an efficient HDGP.

The utilization of hybrid renewable power generation (HRPG) systems is expanding because of their benefits, such as enhanced reliability, security, and stability in electricity supply [17], improved productivity [18], mitigated pollution and environmental impacts [19], and contributions to decarbonization goals [20]. The design and management of isolated renewable microgrids pose significant optimization challenges, particularly in terms of excess energy management, component sizing, and system reliability. These challenges further intensified in cold-climate environments, where seasonal demand variability and extreme temperatures create additional operational constraints, which are not addressed in most of the existing literature [21–23]. HRPG systems are widely deployed in remote, isolated communities and islands to provide electricity needs [24,25]. Recent studies by Shahverdian et al. [26,27] investigated hydrogen-based hybrid renewable systems for off-grid applications, demonstrating that integrating photovoltaic (PV) and ground-source systems, proton exchange membrane fuel cells, and hydrogen storage with multi-objective optimization can improve the reliability, sustainability, and economic feasibility of HRPG systems. These findings further support the motivation of the present HDGP study.

The design of HRPG systems depends on multiple factors, comprising local and regional characteristics (e.g., weather, geographical, and geological attributes) [28,29], resource availability and existing infrastructure (e.g., transmission lines) [30], along with energy demand, and load profile and variability [31,32].

Studies demonstrate the potential of hybrid renewable energy systems (HRESs) to improve reliability, reduce emissions, and enhance techno-economic performance in remote and energy-intensive applications. Wang and Simonson [33] reported that a grid-tied PV system for poultry farms achieved an optimal PV capacity of 20 kW and reduced the net present cost (NPC) by about USD$ 3200 compared with the no-PV base case, although battery storage was not economically feasible under current market conditions. Mahmoud et al. [34] optimized a hybrid PV-concentrated solar power (CSP) plant and found that the optimal configuration, consisting of 61.4% PV and 38.6% CSP, produced 3.64×10^8 kWh/year with a levelized cost of electricity (LCOE) of USD$ 0.033/kWh. In geothermal applications, Hajabdollahi et al. [35] showed that a geothermal-based cogeneration system achieved an exergy efficiency of 23.81% and a payback duration (PD) of ~7 years, confirming its technical and economic viability. Similarly, Salari et al. [36] demonstrated that a wind–diesel–battery HRES for remote communities reduced annual CO_2 emissions from 72,500 to 15,190 kg/year and diesel consumption from 29,970 to 5854 L/year. These findings further support the development of optimized geothermal-based hybrid systems (GBHSs) for reliable, low-carbon, and economically feasible power generation, consistent with the objective of the present research. HRPG systems incorporating GE have been investigated from various perspectives and for different applications. However, GBHSs have generally received less attention compared to other hybrid system combinations. Olabi et al. [37] examined various potential integrations of GE with other energy sources and technologies to enhance output productivity. Their findings demonstrate that geothermal-solar integration is the most common combination. Moreover, only about one-eighth of GBHSs are dedicated to producing electricity. Kariuki et al. [38] conducted a systematic review of hybrid geothermal-solar power systems, examining their trends, challenges, opportunities, and prospects. While these systems offer various benefits and applications, their complexity remains a major issue due to the need for advanced control and optimization, as well as economic and feasibility assessments, along with design, operational, and maintenance challenges. A study by Bokelman et al. [39] found that a hybrid power system combining geothermal and solar can generate 2 to 9 times more electrical energy than a stand-alone geothermal-based binary cycle system.

Using Aspen-HYSYS software, Zhou et al. [40] evaluated the operation and effectiveness of a hybrid solar-geothermal system based on LCOE and power output, comparing it to stand-alone solar and geothermal systems located in a hot, dry region of Australia. They examined the impact of key controlling factors, encompassing ambient air temperature, solar radiation, geo-reservoir quality, and the power cycle's steady and unsteady operating modes. Their findings indicate that the hybrid system outperforms stand-alone geothermal and solar systems when at least 68% of its energy input is derived from solar energy. Moreover, the LCOE of the hybrid system was about 23% lower than that of the stand-alone geothermal installation. According to a techno-economic, environmental, and site appropriateness assessment conducted by Fedakar et al. [41] in three provinces in Türkiye, hybridizing geothermal and solar energy results in approximately 64% lower carbon dioxide emissions and a significantly lower LCOE compared to stand-alone solar PV systems with a suitably sized battery bank.

Hai et al. [42] studied the hybridization of geothermal and biomass energy via two different approaches to enhance electricity production in a gas turbine-Rankine cycle combined power plant. Tafavogh and Zahedi [43] proposed an innovative hybrid system that encompasses five renewable sources—geothermal, solar, hydro, wind, and biomass—to provide electricity, heat, and pure water. Bozkurt and Genç [44] analyzed and optimized a hybrid geothermal-solar-wind power system using HOMER™ software. Naseh and Behdani [45] carried out a feasibility analysis on a hybrid geothermal-solar-wind-diesel power system to define the optimal size for both off-grid and grid-connected utilizations. Bamisile et al. [46] modelled and analyzed a hybrid wind-geothermal system (using the Kalina cycle) for multi-generation uses, such as electrical power and hydrogen production, utilizing a novel technique. Nuclear and geothermal energy are hybridized to produce hydrogen through three separate cycles, alongside the generation of electrical and thermal energy [47]. Liu et al. [48] analyzed an innovative hybrid system integrating geothermal and biogas for the concurrent production of electrical power (using the binary cycle), hydrogen, and fresh/hot/cold water utilizing Aspen-HYSYS software.

Beyond cold-environment and geothermal-centric configurations, HOMER™-based techno-economic optimization has also been widely applied to design off-grid and grid-connected HRPG systems in tropical, developing-country settings, offering useful methodological parallels for the present work. Yadav et al. [49–51] emphasized the role of HOMER™-based optimization in improving the techno-economic performance of isolated HRESs. Their studies considered hybrid renewable configurations with multi-energy storage [49], isolated rural microgrid design [50], and techno-economic-environmental energy management using different storage technologies [51]. Mojumder et al. [52] coupled HOMER™ Pro with MATLAB/Simulink to evaluate PV–wind–battery–grid microgrids in Hatiya Upazila, Bangladesh, reporting an LCOE of 0.0587 USD$/kWh alongside a life-cycle assessment of environmental impacts. Related studies have extended this approach to PV/wind/diesel/battery hybridizations for rural Char Atra [53], rooftop PV systems for an urban campus [54], and PV–biomass–battery configurations for Char Amanullah [55], while broader reviews [56,57] have situated such designs within global HRES challenges, regulatory frameworks, and battery-recycling sustainability concerns. Although these studies address warm, tropical contexts, they collectively demonstrate that HOMER™-based multi-source optimization, fuel- and resource-sensitivity analysis, and life-cycle-aware design constitute a transferable methodological framework—one that this research adapts to the very different climatic, geological, and load-profile constraints of a remote northern Canadian community served by an HDGP.

Momani et al. [58] applied an artificial rabbit optimization for the cost-optimal sizing of battery energy storage systems in microgrids and achieved a reduction in operational cost from 1069.10 USD$/day to 778.81 USD$/day. Similarly, Alsaqqar and Abuelrub [59] utilized particle swarm optimization and golden jackal optimization algorithms for optimizing hybrid PV-diesel-hydrogen systems, showing that higher renewable energy penetration significantly reduced CO_2 emissions, although it increased the total NPC by ~39%. These studies demonstrate the importance of integrating advanced optimization algorithms and techno-economic assessment in the design of reliable HRESs.

Geothermal-based power plants (alone or combined with other sources and technologies) in cold environments have received fewer investigations and implementations than those in hot/warm environments. There are several geothermal-based power plants in cold-climate countries, such as Iceland and Alaska (USA), which operate as stand-alone geothermal facilities, while in Canada, a hybrid geothermal-natural gas system is in operation [60]. One of the primary contributions of this research in filling knowledge gaps is the techno-energy-economic assessment of the long-term (30+ years) performance of HDGP utilization in a cold and harsh environment (Canada's north), with a focus on clean energy access and security for the benefit of local inhabitants.

Canada, as a cold, expansive, and energy-intensive country, stands among the highest per capita energy consumers globally [61]. Its various regions utilize diverse energy sources to produce both electrical power and heat [62]. The country is also home to many (>280) remote (i.e., off-grid) communities, primarily Indigenous and sparsely populated [63], plus isolated sites, e.g., mines and military bases. They are predominantly situated in Canada's north and rely heavily, or entirely, on CBNR energy sources (largely diesel, but also oil and coal) to fulfill their electrical power and heating requirements [16], with an annual consumption of about 90 million litres of diesel fuel [64]. Canada plans to achieve carbon neutrality by 2050 [65]; as part of this plan, the country is working to lessen its dependence on fossil fuel-based facilities (primarily diesel systems) in remote communities and isolated sites by developing cleaner and more eco-friendly energy sources. GE, whether stand-alone or hybridized, is a promising renewable and reliable energy source to support this transition, coupled with sustainable and decarbonization practices.

This research aims to assess the feasibility of utilizing an HDGP to meet the annual electrical power requirements of an off-grid, Indigenous, and fossil fuel-reliant community in northern Canada, which is considered representative of similar communities in cold environments globally. Table 1 briefly compares the contributions of the present work with those of selected previous studies. The research's originalities are summarized as follows:

- Determining practical and realistic values for the LCOE and key economic indicators—NPC, net present value (NPV), PD, and internal rate of return (IRR)—by collecting actual data/characteristics of the study area, along with real market prices for the purchase and costs for installation, operation, and maintenance of various hybrid system components.
- Applying a systematic method for the techno-energy-economic performance assessment of an HDGP in a cold climate, incorporating the

Table 1
Comparative literature review of selected hybrid geothermal and renewable energy studies and the present research.

Ref.	System/Scope	Key Findings	Research Gap/Limitation	Contribution of the Present Research
Olabi et al. [37] and Kariuki et al. [38]	Reviews of GBHSs	Geothermal hybridization improves reliability, sustainability, and system performance	Limited detailed techno-economic feasibility assessments and optimization studies	Provides a comprehensive techno-energy-economic feasibility assessment of an HDGP using HOMER™ and COMFAR™
Bokelman et al. [39], Zhou et al. [40], and Fedakar et al. [41]	Geothermal–solar hybrid systems with LCOE analysis	Hybrid systems can reduce LCOE and improve electricity generation compared with stand-alone systems	Limited integration of multi-source systems and project-level economic indicators	Evaluates a multi-source HDGP integrating geothermal, PV, wind, battery storage, and backup systems with detailed financial indicators
Hai et al. [42], Tafavogh and Zahedi [43], Bamisile et al. [46], and Liu et al. [48]	Multi-source GBHSs	Hybrid renewable systems improve energy utilization and operational flexibility	Primarily focused on thermodynamic or conceptual analyses rather than practical feasibility assessment	Focuses on practical implementation using actual load demand, market-based costs, and long-term operational analysis
Bozkurt and Genç [44] and Naseh and Behdani [45]	HOMER™-based geothermal hybrid optimization studies	HOMER™ is effective for identifying optimal hybrid renewable configurations	Limited methodological development for geothermal modelling and integrated economic evaluation	Introduces an innovative HOMER™ geothermal modelling approach combined with COMFAR™ economic analysis
Present research	An HDGP system consisting of PV, wind, battery storage, and diesel backup	Optimized HDGP achieves reliable electricity generation with a lower LCOE than diesel-based systems and favourable NPV, IRR, and PD	-	Provides an integrated techno-energy-economic feasibility framework using actual site data, real market costs, and long-term performance assessment

optimal capacities of wind and solar systems to generate ~50% of the community's electrical power demand. This method ensures the geo-reservoir's thermal energy effectiveness and sustainable productivity during the hybrid plant's operational life.

- Addressing knowledge and research gaps associated with geothermal-based hybrid electrical power generation systems in which GE serves as the leading energy source. Such systems have been less studied and implemented in cold and harsh environments compared to hot/warm environments and other hybrid system configurations.
- Predefining the geothermal system in HOMER™ software through an innovative technical method for modelling and assessment, since this system is not defined in the software in the same manner as other energy-producing technologies.

2. Study area description

To examine the performance of an HDGP designed for a cold environment, the Fort Liard (FL) area was selected as the study site. It is located in the southwest corner of Canada's Northwest Territories (CNT; Fig. 1) and is home to ~500 members of the Acho Dene Koe First Nation. FL's latitude and longitude are, respectively, 60° 14′ 06″ N and 123° 28′ 58″ W. The community's peak power load is ~550 kW [66], while its average power production is ~245 kW [16]. Currently, three diesel generators operate in FL, collectively possessing a capacity of 1.32 MW [67]. One generator serves to provide the baseload, another is designated for automatic-start peak shaving, and the third is utilized as a backup [68]. Fig. 2 presents FL's climatic data, including ambient air temperature (measured at 2 m above the ground), wind speed (at an altitude of 80 m), and solar radiation (both direct and diffuse irradiance), recorded hourly during the year 2019, as an example [16]. The highest and lowest air temperatures are 26.64 °C and −38.05 °C, respectively, with a mean of about −1.9 °C (Fig. 2(a)). In addition, the highest and lowest wind speeds are, respectively, 12.55 m/s and 0.29 m/s, with an average of about 4.3 m/s (Fig. 2(b)).

Each year, FL consumes nearly 550,000 litres of diesel fuel [69], which must be transported during the warmer months from different cities, such as Edmonton in Alberta (~1250 km from FL), Canada. Excluding government subsidies—provided to lessen the LCOE for northern inhabitants—residential energy prices between September and March are ~0.31 CAD$/kWh for the first 1000 kWh per month and above, rising to ~0.70 CAD$/kWh (actual price). In contrast, the subsidized rate applies only to the first 600 kWh/month between April and August [67].

In line with the Government of Canada's objectives for sustainability, decarbonization, and energy security, federal, provincial/territorial, and regional/local governments aim to expand renewable, reliable, and affordable energy systems (stand-alone or hybrid) for remote communities. FL is located within the Western Canadian Sedimentary Basin [70] and sits above a hot sedimentary aquifer, thus a promising site for geothermal power generation [71]. The region's geothermal gradient is around 40 °C/km [72] and its permafrost thickness is about 10 m [73].

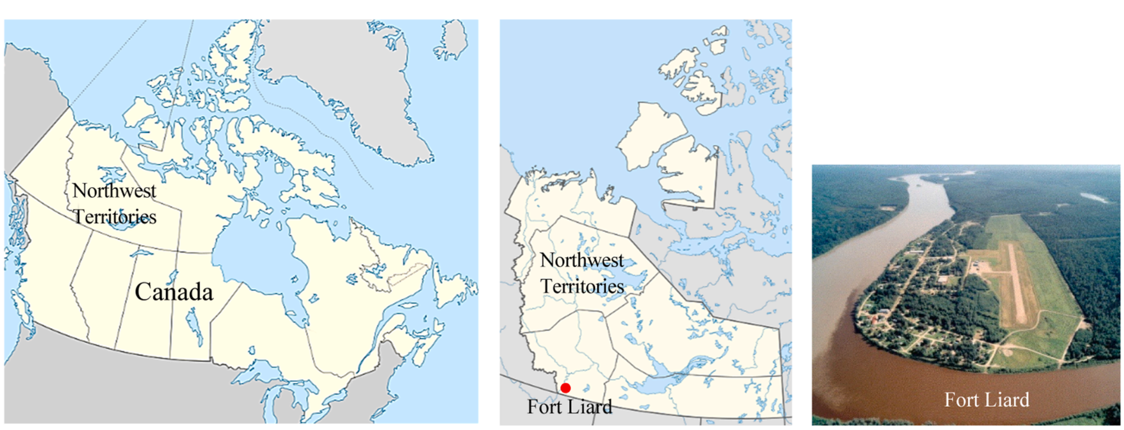

Fig. 1. Map illustrating FL's geographical location within CNT.

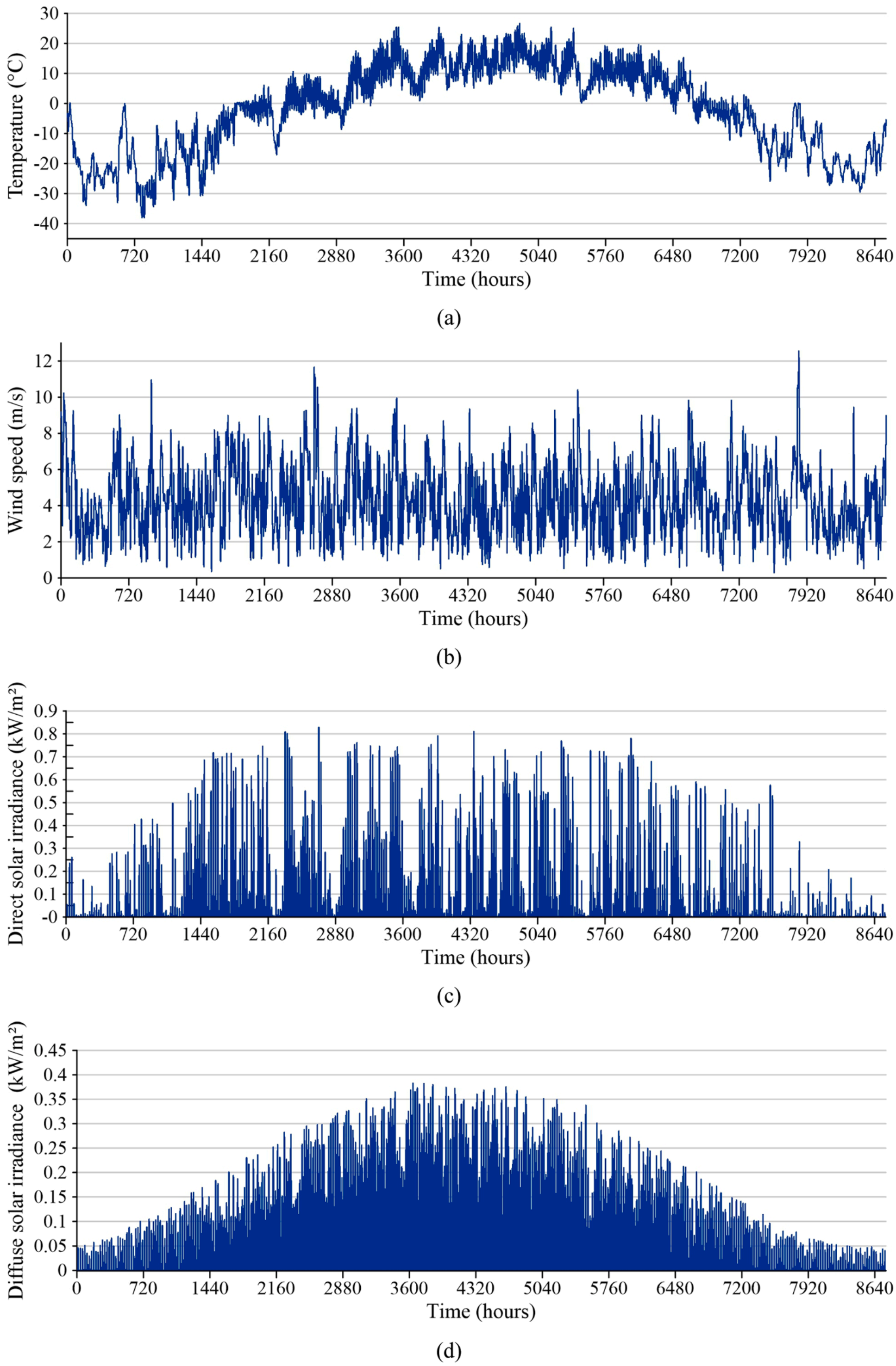

Fig. 2. Changes in (a) ambient air temperature (at 2 m above the ground), (b) wind speed (at 80 m altitude), (c) direct solar irradiance, and (d) diffuse solar irradiance, recorded hourly throughout 2019 in FL, CNT.

In 2011, a Canadian company conducted a preliminary study on developing a stand-alone geothermal system in FL to supply its annual electricity requirements [72]. The geology beneath FL is complex with overlapping terms. The Middle Devonian strata beneath the FL area comprise the Nahanni Formation, underlain by the Headless and Landry Formations. Secondary replacement dolomitization produced the stratigraphically equivalent Manetoe Formation dolomite, as shown in Fig. 3 [72]. The production interval is referred to here as the Nahanni/Manetoe Formations.

The proposed geothermal system consisted of a production well, completed in the Nahanni/Manetoe Formations at a depth of ~4.25 km, and an injection well, planned for shallower the Mattson Formation at a depth of ~1.45 km. The Mattson Formation was selected for re-injection to reduce drilling expenses and mitigate potential issues such as thermal short-circuiting and premature geo-reservoir cooling.

In this research, based on FL's peak electrical power consumption and the worst-case ambient conditions—namely, the warmest expected days of the year happening in June and/or July—a geothermal plant

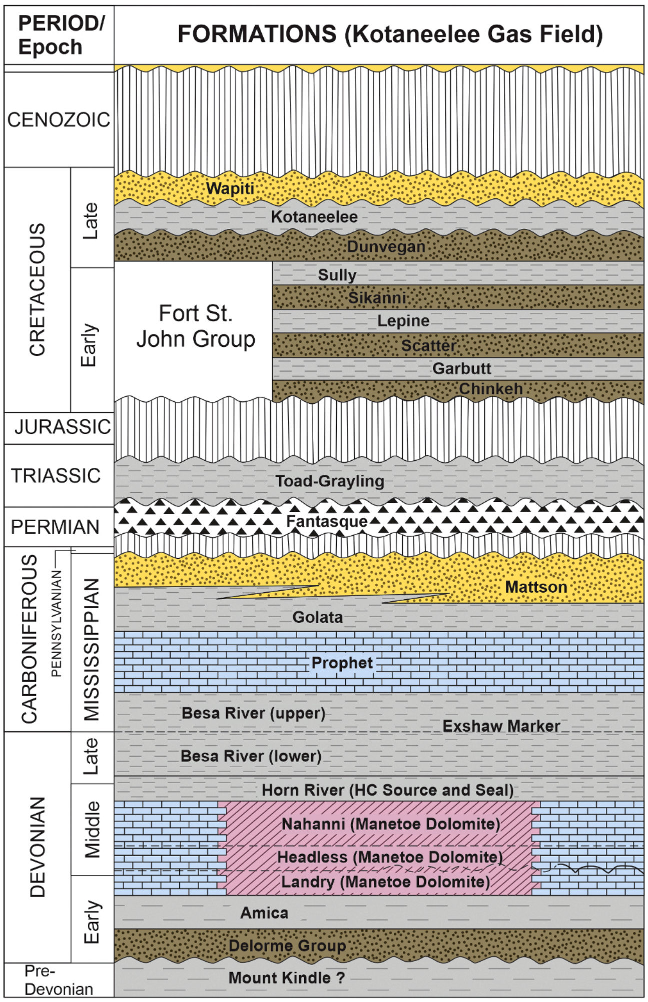

Fig. 3. Stratigraphic column of the geology beneath the FL area (redrawn from [72]). The Manatoe Dolomite is a regionally extensive diagenetic replacement dolomite.

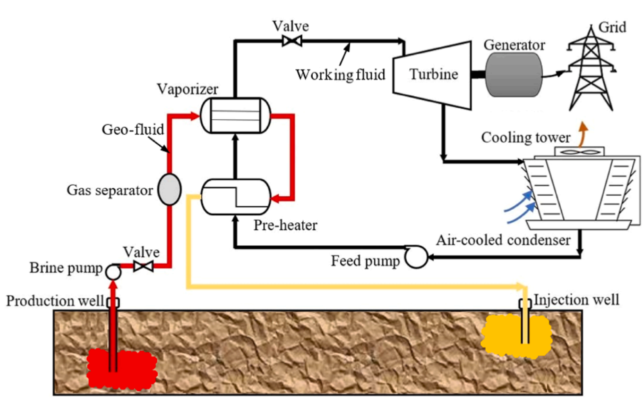

Fig. 4. Schematic design of the single-stage binary ORC geothermal plant (not to scale).

(Fig. 4) was designed as the principal generation source to produce its long-term electricity requirements (30+ years), supplemented by other energy systems. Fig. 4 provides a schematic illustration of the binary organic Rankine cycle (ORC) geothermal plant configuration used as the conceptual basis for the HOMER™ geothermal generator model in this research.

The main input data from the geo-reservoir in the Nahanni/Manetoe Formations to the geothermal plant heat exchanger are as follows:

- Geo-fluid temperature: 170 °C
- Geo-fluid pump pressure: 1200 kPa
- Geo-fluid mass flow rate: 30 kg/s
- Geo-fluid content: Hypersaline fluid (200 ppt) with a neutral pH, high magnesium, calcium, and bicarbonate content, and a sodium-chloride composition [74].

3. Materials and methods

3.1. Simulation and optimization process

The techno-energy-economic feasibility assessment was carried out by applying two software tools—HOMER™ and COMFAR™—to analyze the performance and effectiveness of an HDGP designed specifically for the conditions in FL. Fig. 5 illustrates the process of conducting the feasibility assessment using HOMER™ and COMFAR™. In the first step, real community data—such as power profile and loads, population, climate conditions, geographical features, geological settings, and existing power systems and infrastructure—were collected. Prices for purchasing and costs for installing, operating, and maintaining various HDGP components were also obtained in detail from manufacturers, vendors, and relevant companies; engineering calculations and estimations were used when this information and data were unavailable. Financial indicators, including discount and inflation rates, were also determined. The inflation rate was set at 7.7% and the discount rate at 2.5% [16], reflecting actual values at the time of the assessment (year 2023). The project's lifetime was selected as 30 years, which is a common timeframe for geothermal power plant projects [75,76].

The data transfer between HOMER™ and COMFAR™ proceeds as follows: HOMER™ is used to identify the optimal system configuration and compute the LCOE and NPC under the specified sensitivity parameters. The LCOE output from HOMER™, combined with the actual energy selling price in FL (0.70 CAD$/kWh, unsubsidized [67]), determines the annual revenue stream. Fixed investment costs, operation and maintenance (O&M) costs (Table 3), and replacement schedules derived from HOMER™ optimization results are then entered into COMFAR™ as annual cash flows. COMFAR™ applies standard discounted cash flow methodology [77,78] to compute NPV, IRR, and PD. Validation of the HOMER™ model was performed by comparing the simulated annual energy output against the community load data [66, 67].

In the second stage, all required data and information, along with the HDGP components and their specifications, were entered into HOMER™ for simulations and optimization. Fig. 6 demonstrates the schematic design of the HDGP in HOMER™ based on FL's characteristics. In the third step, COMFAR™ was employed to define the project's economic outcomes, utilizing financial standards. Finally, sensitivity analyses were conducted on several important parameters. FL's total annual electrical energy demand is ~2147 MWh, with peak use occurring in December and January and the lowest in June and July.

A hydrogen system was initially considered as part of the HDGP. HOMER™ simulations indicated that hydrogen-integrated configuration produced a higher LCOE than the optimal HDGP configuration without a hydrogen system, due to the high capital cost of the electrolyzer and fuel cell stack, low round-trip efficiency, and the limited electrical contribution relative to the battery system. The hydrogen system was therefore excluded from the final HDGP design, while it is retained in Fig. 6 to document the full configuration space evaluated.

To realistically simulate demand, daily and hourly random variables (including hourly efficiency) were increased by 10%. This created significant fluctuations in the hourly and daily electrical power profiles. These ±10% variabilities were modelled using real 2020 FL load data. Although actual records show a maximum monthly variation of about 15%, compounding the 10% daily and hourly variables establishes a

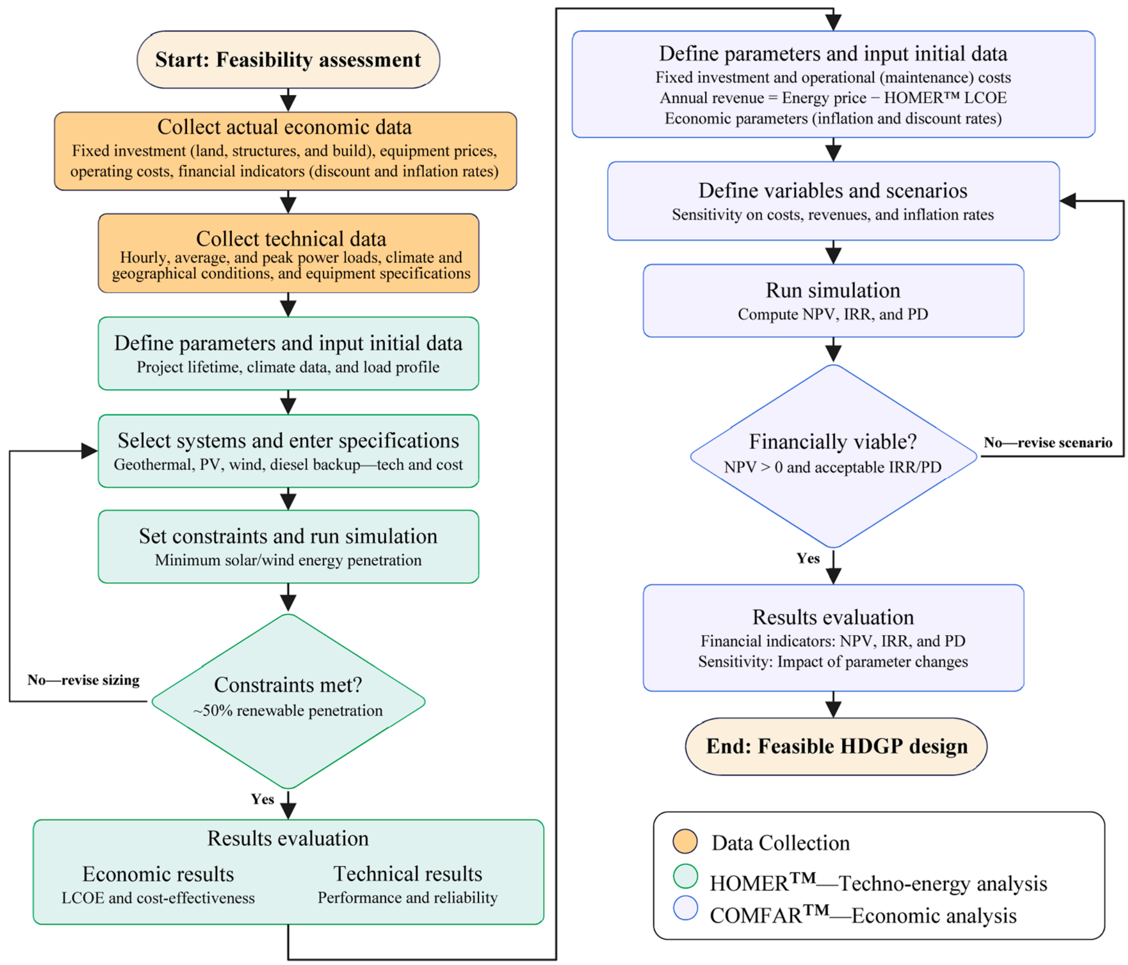

Fig. 5. Feasibility assessment process utilizing HOMER™ and COMFAR™.

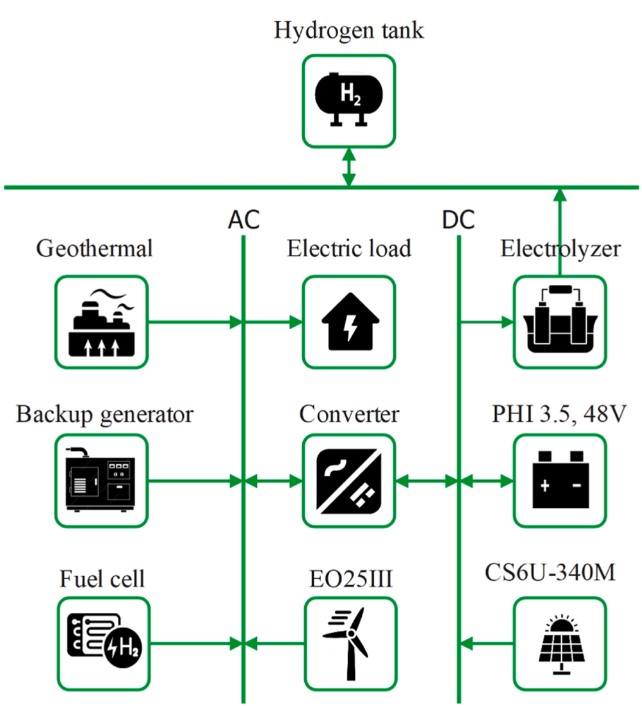

Fig. 6. Schematic design of the proposed HDGP in HOMER™.

conservative "worst-case" fluctuation of roughly 21%. These changes led to noticeably greater variability in both the hourly and daily electricity demand profiles. As a result, the total annual electrical energy demand for the FL community was estimated at approximately 2147 MWh [16], with peak consumption occurring in December/January and the minimum in June/July. Fig. 7 illustrates the changes in hourly and daily electrical power use in FL during the selected year 2020.

The designed HDGP comprises the following components:

- A single-stage binary ORC (the primary source), whose main components consist of a turbine-generator (with an overall efficiency of 77%), an air-cooled condenser (including eight fans), a feed pump, and a heat exchanger incorporating a preheater and a vaporizer with a pinch-point temperature of 8 °C (Fig. 4). The working fluid used in this cycle was R245fa due to its favourable properties.
- Wind turbines (Eocycle EOX25 Class III) with a rated power of 25 kW, a 30-year lifetime, an operating temperature range of −20 to 40 °C, and a cut-in/cut-out wind speed range of 2.75 to 20 m/s.
- PV panels (Canadian Solar CS6U-340 M) with a nominal maximum power of 340 W, a 25-year design lifetime, a module efficiency of 20.2%, and an operating temperature range of −40 to 85 °C.
- A battery storage system (BSS) comprising SimpliPhi PHI 3.8 kWh 48 V lithium batteries with a 25-year lifetime, an operating efficiency of 98%, and an operating temperature range of −20 to 60 °C. To ensure appropriate operating conditions for the battery bank, a winterized container was used.
- A converter with a lifetime of over 15 years and an efficiency of 96.5%.

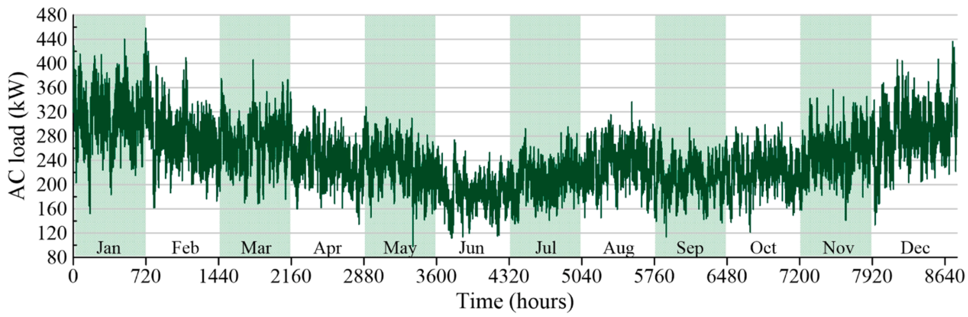

(a)

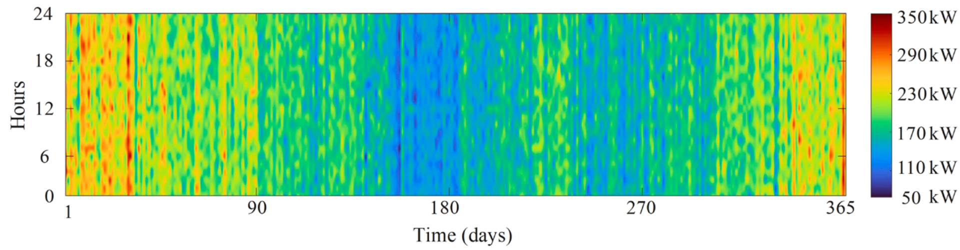

(b)

Fig. 7. (a) Hourly and (b) daily electrical power consumption changes in FL during 2020.

- A backup diesel generator (for emergencies, maintenance, and repair periods only).

The above components were selected from a range of commercially available options based on their suitable specifications. The battery bank serves as both an energy storage medium and an uninterruptible power supply (UPS) for 30 min. The 30-minute UPS specification corresponds to the estimated ORC plant ramp-up time from minimum output (~10 kW, 1% of rated capacity) to full net output (~600 kW), governed by the thermal inertia of the binary cycle heat exchanger. This duration also exceeds the diesel generator emergency startup time (around 5–10 min), ensuring a seamless transition to backup operation if required.

3.2. Sensitivity analysis process

To maintain the geo-reservoir's thermal energy effectiveness and ensure its sustainable productivity throughout the HDGP's 30-year operational life, sensitivity analyses conducted using HOMER™ for various wind and solar system capacities (shown in Table 2) identified their optimal capacities as ~50% of FL's electrical power requirements, considering the lowest LCOE while mitigating the geo-reservoir's thermal capacity degradation. Indeed, HOMER™ simulates and analyzes systems based on the entered capacities. For each scenario, nearly 1500,000 individual simulations are performed. Table 3 presents the capacity of each component in the designed HDGP according to HOMER™'s optimization results.

Based on the calculations conducted [16], the geothermal plant's net electrical power output is ~600 kW, which exceeds FL's peak electrical power demand (~550 kW), occurring only on a few hours/days each year. The remaining electrical power output (~400 kW) is allocated for the plant's own operations. The average hourly meteorological data—such as global horizontal irradiance, wind speed, and ambient air temperature—for a 30-year period were used in HOMER™, based on FL's geographical coordinates derived from the NASA dataset.

This research reasonably assumes that the selected geo-reservoir for geo-fluid extraction in the dolomite strata of the Nahanni/Manetoe Formations are capable of retaining consistent geo-fluid temperature at a relatively low flow rate (30 kg/s) during the project's lifetime for several reasons, as outlined below:

- Integrating wind and solar systems to provide ~50% of the community's annual electrical power demand.
- The presence of suitable thermo-fluid and geological properties, as determined from 50 offset deep oil and gas wells within a 30 km radius of FL. The obtained data illustrate that the target geo-reservoir possesses high temperatures (~178 °C at the top and ~184 °C at the

Table 2
Sensitivity analyses conducted using HOMER™ for various parameters and components.

Parameter/ component	Unit	Amount
Inflation rate	Percent	3, 5, 7, 7.7, and 9
Global horizontal irradiation	kWh/m^2/ day	2, 2.5, 2.89, 3, 3.5, and 4
Wind speed	m/s	2, 2.5, 3, 3.33, 3.5, 4, and 4.5
Geothermal plant	kW (capacity)	1000
Wind turbines	kW (capacity)	0, 100, 200, 300, 400, 500, 600, 700, 800, 900, 1000, 1100, 1200, 1300, 1400, 1500, 1600, 1700, 1800, 1900, and 2000
PV panels	kW (capacity)	0, 100, 200, 300, 400, 500, 600, 700, 800, 900, 1000, 1100, 1200, 1300, 1400, 1500, 1600, 1700, 1800, 1900, and 2000
Backup generator	kW (capacity)	500
Battery bank	String	100, 200, 300, 400, 600, 900, 1200, 1500, 1800, 2100, 2400, 2700, and 3000

Table 3
Capacity of components in the HDGP based on HOMER™'s optimization results.

Component	Capacity	Unit
Geothermal plant	~1000	kW
Wind turbines	16	#
PV panels	400	kW
Backup generator	500	kW
Battery bank	200	string
Converter	288	kW

bottom [72]); high permeability and porosity (ranging from 5% to 12%, measured from drill cores [79]); significant geo-fluid influx because of its liquid-dominated nature; and a highly fractured geological structure.

- A geo-reservoir volume of 3.75 km^3 and a thickness of ~150 m beneath the study community [72].
- Sustainability calculations for the target geo-reservoir, considering a 15% thermal energy recovery factor and 9% electrical efficiency, which demonstrated its ability to generate electricity for 30 years [16,72].

Accurately characterizing a geo-reservoir generally involves several essential steps. These typically include drilling a test well, doing temperature logging and flow tests, and simulating the reservoir's thermal and chemical behaviour over the entire project lifespan.

Table 4 provides the fixed investment expenditures, comprising prices for the selected equipment and preparatory expenses (transportation expense, site preparation expense, etc.), accompanied by the O&M expenditures. O&M expenditures are calculated on an annual basis. For the geothermal plant, the O&M expense is determined and reported per unit of annual operating hours. The geothermal plant capital cost of ~18.2 million CAD$ includes drilling and completion of both production and injection wells, the binary ORC, and associated surface infrastructure. Drilling operations constitute the largest portion of the investment (~16 million CAD$), while the remaining costs correspond to engineering design, procurement, site preparation, civil works, and installation of surface equipment. These costs were estimated using actual market-based geothermal project cost data and supplier quotations.

3.3. Governing equations

3.3.1. Geothermal system

An innovative technical approach was utilized to simulate the geothermal system in HOMER™ since it is not predefined in the software like wind and solar systems. Hence, the geothermal system was modelled as a generator with a specific fuel (i.e., geo-fluid or brine) in the software. The calorific value of this new fuel, LHV_{gf}, can be obtained from Eq. (1) [80], based on the brine's specific heat capacity, $C_{P,gf}\left(\simeq 3.8\frac{\text{kJ}}{\text{kg}}{}^{\circ}\text{C}\ [16]\right)$, and the brine temperature difference between the inlet and outlet of the heat exchanger (see Fig. 4), ΔT_{gf} ($\simeq 60.26\ ^{\circ}C$)—the data is sourced from [16].

$$LHV_{gf} = C_{P,gf}\ \Delta T_{gf} \tag{1}$$

The resulting calorific value ($LHV_{gf}\ =\ \sim 0.229$ MJ/kg) and the brine density ($\rho_{gf}\ = 897\frac{kg}{m^3}$ [16]) are employed to define a new fuel in HOMER™'s library, referred to as "brine-fuel." After defining the specific fuel, a ~1000-kW generator was selected as the geothermal system, which can be described as a "brine-fueled generator system."

The brine-fuel consumption (L/kWh) represents the amount of fuel (brine) required to generate 1 kW of gross electrical power for one hour.

Table 4
Fixed investment and O&M expenditures for each HDGP equipment.

O&M cost (CAD $/yr)	Fixed investment cost (CAD$)	Equipment
125,000	18,210,000	Geothermal plant
64,000	6560,000	Wind turbines
10,741	787,094	PV panels
5/operation hour	150,000	Backup generator
200	760,000	Battery bank
-	207,624	Converter
1000	20,000	Other fixed investments (e.g., winterized container)

To establish the formulation, it is necessary to determine the total thermal power production and the volumetric flow rate of fuel.

$$\text{Total thermal power production}_{gf} = \dot{m}_{gf}\ C_{P,gf}\ \Delta T_{gf} \tag{2}$$

where $\dot{m}_{gf}\left(=30\frac{kg}{s}\right)$ is the mass flow rate of geo-fluid.

Applying Eq. (2) yields a total thermal power production of ~6.87 MW, which represents the heat exchange between the geo-fluid and the working fluid inside the heat exchanger.

The volumetric flow rate is given by:

$$\text{Volumetric flow}_{gf} = \frac{\dot{m}_{gf}}{\rho_{gf}} \tag{3}$$

Applying Eq. (3) yields a volumetric flow rate of ~120,401 L/hr, indicating that the volume of brine-fuel must flow through the heat exchanger to produce ~6.87 MW of thermal power. By dividing the volumetric flow rate by the total thermal power production, the brine-fuel consumption can be determined as follows:

$$\text{brine} - \text{fuel consumption} = \frac{\text{Volumetric flow}_{gf}}{\text{Total thermal power production}_{gf}} \tag{4}$$

Applying Eq. (4) yields a brine-fuel consumption of ~17.53 L/kWh; that is, the geothermal system consumes ~17.53 litres of brine-fuel per kWh of gross electricity generated. This value is used to define the brine-fuel in HOMER™.

Within the operational framework considered in this research, it is assumed that the geothermal system can operate continuously with a minimum net output corresponding to 1% of its rated capacity, ensuring stable baseload operation. If electricity consumption increases or wind and solar PV generation drops, the geothermal system automatically adjusts its output to supply the community's electrical power needs.

3.3.2. Battery storage system (BSS)

A BSS is integrated into the hybrid system to improve operational flexibility and mitigate the intermittency associated with renewable energy generation. The charging and discharging behaviour of the battery bank is governed by the balance between renewable generation, load demand, system control strategy, and the battery state of charge (SOC).

The battery system's performance and lifetime are strongly influenced by the depth of discharge (DOD) and operating temperature. The DOD characterizes the proportion of the total battery capacity that can be safely utilized during operation. Accordingly, the minimum allowable SOC can be expressed as:

$$SOC_{min} = 100 - DOD \tag{5}$$

Based on the manufacturer's specifications for the selected battery technology, a DOD of 90% was adopted in this research, and subsequently, $SOC_{min}\ =\ 10$. This constraint prevents excessive battery degradation and contributes to reliable long-term system performance.

3.3.3. Component operational lifecycle

The operational lifecycle of each system component represents the duration over which it can operate reliably under standard operating conditions before replacement is required. Within the HOMER™ modelling framework, the component lifecycle is associated with annual operating hours and the overall project lifetime. The effective operational lifecycle can be estimated as [81]:

$$\text{Operational lifecycle} = \frac{\text{Project lifetime (hours)}}{\text{Annual operating hours}} \tag{6}$$

The above equation enables the determination of component replacement intervals, which are subsequently incorporated into the techno-economic assessment of the hybrid system.

3.3.4. Economic performance indicators

The economic feasibility of the designed HDGP is assessed utilizing several widely adopted financial indicators, including NPC, LCOE, NPV, IRR, and PD. According to HOMER™, NPC, also known as the life-cycle cost, represents the present value of all expenses associated with installing and operating a power plant throughout its project lifespan, offset by the present value of the total revenue generated during the same period. Considering the inflation rate f, the present value of annual costs is expressed as [82]:

$$\mathrm{NPC} = \sum_{t=1}^{n} \frac{C_t (1+f)^t}{(1+i)^t} \tag{7}$$

where C_t is the annual cost in year t, i is the nominal discount rate, and n is the project lifetime.

The real discount rate is calculated using the following equation [82]:

$$i_{real} = \frac{i-f}{1+f} \tag{8}$$

The total NPC is converted into an equivalent annual cost using the capital recovery factor (CRF), as follows [83]:

$$CRF(i_{real}, n) = \frac{i_{real}(1+i_{real})^n}{(1+i_{real})^n - 1} \tag{9}$$

The total annualized cost of the hybrid system is therefore [84]:

$$C_{ann,tot} = NPC_{tot} \times CRF \tag{10}$$

The LCOE can be calculated as [84]:

$$\mathrm{LCOE} = \frac{C_{ann,tot}}{E_{served}} \tag{11}$$

where E_{served} denotes the annual electrical load supplied by the system.

The NPV is an economic metric based on the discounted cash flow method that accounts for the inherent time value of money. It is well-suited for the economic assessment of capital-intensive, long-term projects and can establish relationships between profitability, operational efficiency, and environmental performance [77]. The NPV is defined as [78]:

$$NPV = \sum_{t=1}^{n} \frac{C_t}{(1+r)^t} - C_0 \tag{12}$$

Here, C_0 is the initial investment and r is the nominal discount rate.

The IRR is a financial metric employed to estimate the potential return on an investment [85], with a higher IRR making a project more appealing. The IRR corresponds to the discount rate at which the NPV becomes zero [86]:

$$NPV = \sum_{t=1}^{n} \frac{C_t}{(1+IRR)^t} - C_0 = 0 \tag{13}$$

The PD is another key financial metric utilized to evaluate the profitability of an investment. However, it measures different aspects of the investment's financial performance compared to the IRR. The PD represents the time required to recover the initial investment, given by [87]:

$$\mathrm{PD} = \frac{\text{Initial investment}}{\text{Annual cash inflow}} \tag{14}$$

It should be noted that the IRR reflects the investment's profitability over time, while PD provides a snapshot of the total profit relative to the initial cost.

The salvage value of system components at the end of the project lifetime, assuming linear depreciation, is determined by [88]:

$$S = C_{rep} \frac{R_{rem}}{R_{comp}} \tag{15}$$

where C_{rep} is the replacement cost and R_{comp} represents the component lifetime. The remaining lifetime of a component is calculated as [88]:

$$R_{rem} = R_{comp} - (R_{proj} - R_{rep}) \tag{16}$$

The replacement cost duration (R_{rep}), utilizing the integer function $INT()$, is given by [88]:

$$R_{rep} = R_{comp} \cdot INT\left(\frac{R_{proj}}{R_{comp}}\right) \tag{17}$$

Here, R_{proj} is the project lifetime and R_{comp} is the equipment lifetime.

4. Results and discussion

4.1. Techno-energy assessment

Based on the techno-energy results obtained from HOMER™ simulations, Table 5 summarizes the annual electricity production of each HDGP component. The geothermal system's share of total electricity generation (~54%) is consistent with the baseload-dominant design philosophy adopted in this research. This proportion is higher than the 40–45% geothermal contribution reported for hybrid solar-geothermal systems in temperate climates [39,40], which is expected given FL's high-latitude, low-insolation conditions. The wind contribution (~25%) aligns well with the average wind speed of ~4 m/s at 30 m hub height. The PV contribution (~21%) is lower than that reported for lower-latitude hybrid systems [41], reflecting the seasonal solar resource limitations at 60°N. However, PV generation is strategically concentrated during the summer months, when the geothermal system is modulated to its minimum output, thereby maximizing geo-reservoir thermal recovery. Under baseline operating conditions, the HDGP displaces ~550,000 litres of diesel per year [69], equivalent to an annual CO_2 avoidance of ~1450 tonnes CO_2 (using an emission factor of 2.68 kg CO_2/L diesel [89]). Of this reduction, the geothermal system contributes ~783 tonnes CO_2/year avoided (~54%), wind turbines ~362 tonnes/year (~25%), and PV panels ~305 tonnes/year ~ (21%). As shown in Table 4, the geothermal, wind, and solar PV systems respectively produce ~1266, ~588, and ~497 MWh of electrical energy per year, and the total annual electricity produced (~2350 MWh/year) slightly exceeds the yearly electricity demand (~2147 MWh/year) in FL. The primary reason for the surplus electricity production by the HDGP is the alteration in geothermal system utilization throughout the year. This surplus electricity can be employed for various purposes, such as community development through the establishment of greenhouses or passive community heating. Under normal conditions, the backup diesel generator produces no power. It is only activated during emergencies, repair, or maintenance periods. The designed HDGP can serve as a clean and eco-friendly electrical power producer during its operation.

A worst-case reliability analysis confirms that, in the event of simultaneous geothermal plant shutdown and absence of wind/solar generation, the 760-kWh BSS (684 kWh usable at 90% DOD) can supply the residual 50 kW load (peak demand minus generator capacity) for ~13.7 h. The backup diesel generator is activated within about 5–10 min during extended outages. HOMER™ simulations confirmed zero

Table 5
Summary of electricity production by each component in the designed HDGP.

Component	Production (kWh/year)	Percent
Geothermal plant	1265,799	53.9
Wind turbines	588,045	25.0
PV panels	496,606	21.1
Backup generator	0	0
Total	2350,450	100

annual unmet load, validating the system's reliability in meeting FL's electricity demand under all simulated operating conditions.

Fig. 8 displays the electrical power output of each HDGP component over time during a year. As depicted in Fig. 8(a) and (c), the impact of PV panel utilization is evident during the hours between 10 AM and 6 PM, especially in the summer months when solar insolation is at its peak in this region. As demonstrated in Fig. 8, the electrical power produced by the geothermal system fluctuates during daylight hours in response to the performance of the PV panels and wind turbines. When these renewable sources operate efficiently, the geothermal system maintains a minimum output level to preserve its recovery ability and long-term stability. Table 6 shows a summary of the electrical power output for the geothermal, solar PV, and wind systems in the designed HDGP, along with their hours of operation over the course of a year.

Fig. 9 illustrates the charge and discharge cycles of the BSS over time during a year. This storage system, which consists of 200 batteries, is extensively employed to meet FL's electrical power demand. The battery bank helps enhance the stability, reliability, and security of the electrical power supply, enabling it alone to meet FL's electrical power requirements for ~3 h.

For comparison purposes, HOMER™ simulations indicated that if a solar PV system were to independently provide the community's electrical power demands instead of the designed HDGP, approximately 2800 kW of PV panels would be required. In the case of an independent electrical power supply by a wind system, 96 × 25-kW wind turbines (totalling 2400 kW) would be needed. Note that the capacity of renewable systems may vary depending on the rated capacity of the BSS. In both cases, a large number of batteries would be required due to the intermittent nature of wind and solar energy. Calculations conducted using HOMER™ software indicated that the geothermal system requires an annual consumption of 22,170,997 litres of brine-fuel to generate 1265,799 kWh of electricity, with an average brine-fuel consumption of ~2531 litres per hour and ~60,742 litres per day.

Table 6
Summary of electrical power output and hours of operation per annum for the geothermal, solar PV, and wind systems in the HDGP.

Quantity	Geothermal system	PV panels	Wind turbines	Units
Min. electrical power output	6.00	0	0	kW
Max. electrical power output	440	460	540	kW
Ave. electrical power output	208	56.7	67.1	kW
Hours of operation	6095	4394	5263	hours/year

Applying Eq. (6) yields an operational lifecycle of ~43 years for the geothermal plant. This result indicates that the hybrid system proposed in this research can extend the geothermal plant's operational lifecycle from the initial project lifetime of 30 years to ~43 years. This extension is attributed to reduced annual operating hours resulting from the integration of solar PV and wind systems. It further exhibits that the employed hybridization strategy helps preserve the geo-reservoir's thermal energy efficiency and long-term stability. Previous geo-reservoir engineering studies have reported that reducing geothermal production rates and implementing intermittent or moderated utilization strategies can mitigate geo-reservoir thermal drawdown and improve long-term reservoir sustainability [90,91]. Therefore, the calculated ~43-year operational period in the present research should be interpreted as an estimated extension of the system lifecycle associated with reduced geothermal utilization due to hybridization with wind and solar PV systems, rather than as the result of a fully coupled geo-reservoir simulation.

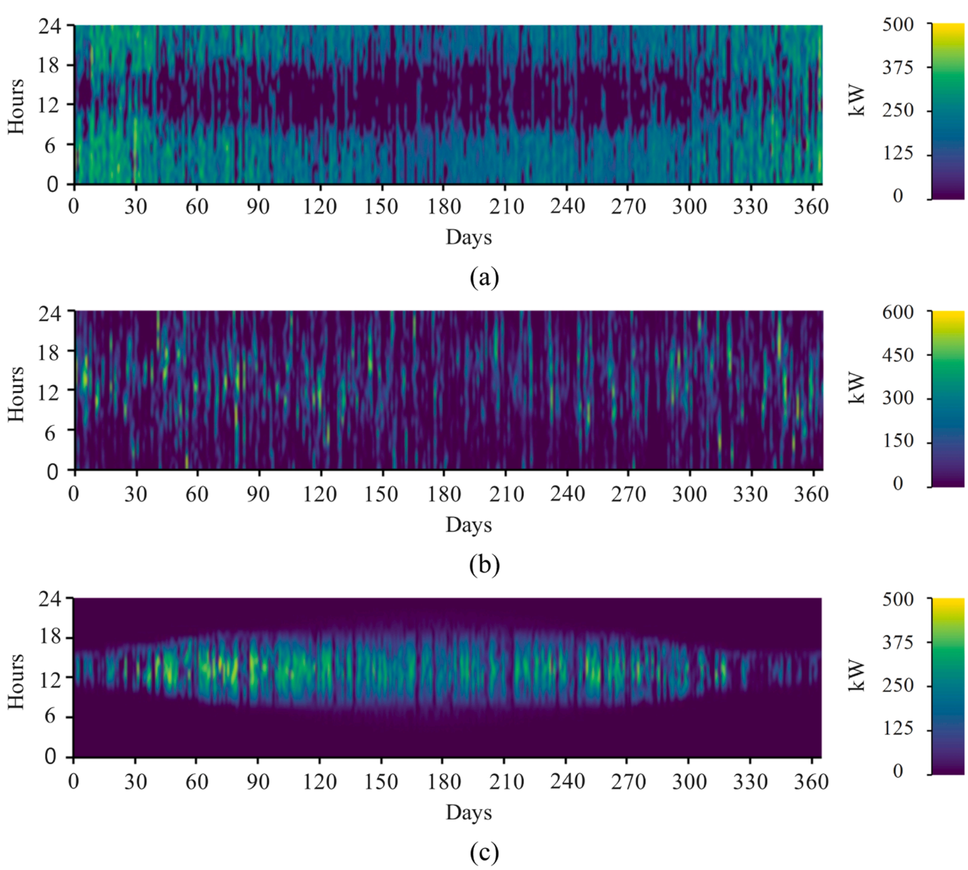

Fig. 8. Variations in electrical power production over time for (a) geothermal, (b) wind, and (c) solar PV systems.

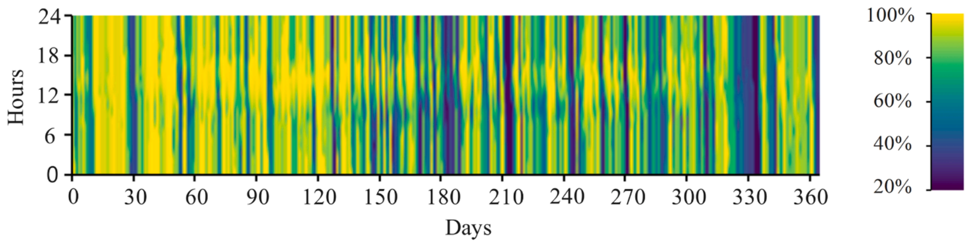

Fig. 9. Charge and discharge cycles of the BSS.

4.2. Economic assessment

To perform the economic assessment utilizing HOMER™ and COMFAR™ software, various factors—including replacement cost, salvage value, and NPC—must first be determined. Table 7 presents the breakdown of NPC for the designed HDGP. The replacement cost accounts for the periodic renewal of HDGP components, whereas the salvage value is calculated based on each component's technical working hours and the remaining nominal lifetime.

The cost summary for the designed HDGP is presented in Table 8. The LCOE for the HDGP is ~0.27 CAD$/kWh, substantially lower than the ~0.70 CAD$/kWh LCOE for the current diesel facility in FL, considering the unsubsidized cost of diesel in northern Canada.

COMFAR™ software uses financial standards to compute various economic indicators, such as the NPV, IRR and PD. The changes in NPV based on a discount rate ranging from 0% to 100% are depicted in Fig. 10. As illustrated in this figure, the NPV at a 0% discount rate is almost equal to CAD$ 137 M, indicating that the initial investment value is fixed at around CAD$ 28 M and will reach CAD$ 165 M after 30 years. When the discount rate is 2.5%, the approximate investment value after 30 years reaches about CAD$ 100 M, meaning that the investment increases by CAD$ 72 M.

Fig. 11 represents the IRR for the designed HDGP, which is calculated to be 10.7%. For comparison purposes, if only the geothermal plant is considered to fulfill FL's electrical power requirements, its IRR is determined to be 14.1%, which is slightly higher than that of the designed HDGP caused by the lower capital investment. However, while the hybrid system has a slightly lower IRR, it can extend the project's lifetime by enabling the recovery and recharge of the geo-reservoir.

The PD for the designed HDGP is shown in Fig. 12 for both normal mode and dynamic mode (calculated at a 2.5% discount rate) and is compared with that of a stand-alone geothermal plant. The PD for the designed HDGP is found to be 12.9 years in normal mode and 14.6 years in dynamic mode, which are slightly greater than those of the stand-alone geothermal system.

4.3. Sensitivity analysis

HOMER™ software was used to perform sensitivity analysis for some selected parameters.

Table 8
Summary of the costs for the designed HDGP (CAD$).

Capital cost	26.7M
Operating cost	11.5M
Replacement cost	18.3M
Salvage value	−16.3M
Total cost	40.3M
LCOE	CAD$0.27/kWh

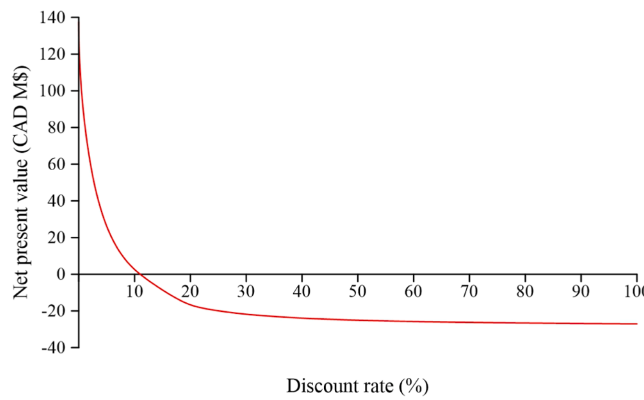

Fig. 10. NPV variations for the designed HDGP, presented in Canadian dollars.

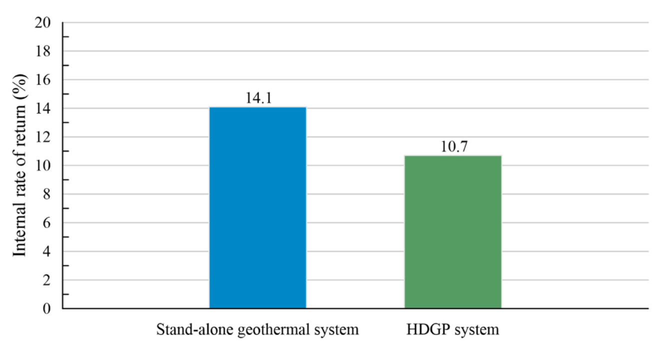

Fig. 11. IRR for the designed HDGP and the stand-alone geothermal system.

Table 7
NPC for the designed HDGP, presented in Canadian dollars.

Component	Capital cost (CAD$)	Operating cost (CAD$)	Replacement cost (CAD$)	Salvage value (CAD$)	Total cost (CAD$)
Geothermal plant	18.2M	6.15M	0.00	0.00	24.4M
Wind turbines	6.56M	4.52M	13.2M	−10.9M	13.5M
PV panels	787,094	759,325	2.03M	−2.08M	1.50M
Backup generator	150,000	0.00	0.00	-$642,123	−492,123
Battery bank	760,000	14,139	2.62M	−2.68M	709,747
Converter	207,624	0.00	436,169	0.00	643,793
Other equipment	20,000	70,693	0.00	0.00	90,693
Whole HDGP	26.7M	11.5M	18.3M	−16.3M	40.3M

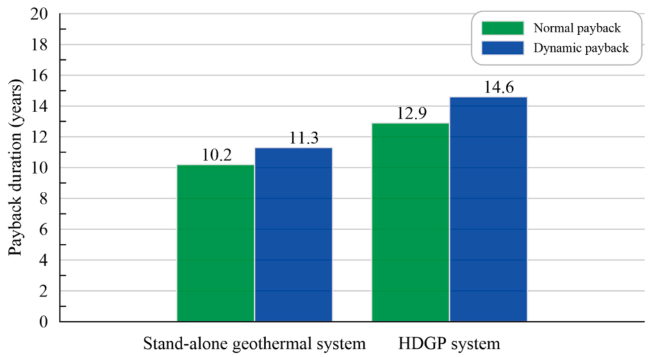

Fig. 12. Normal and dynamic PDs for the designed HDGP and the stand-alone geothermal system.

4.3.1. *Sensitivity analysis of the economic indicators*

According to the sensitivity analysis conducted on the inflation rate, which was examined within the range of 2.5% to 10% (Table 2), the LCOE for the designed HDGP is determined and shown in Fig. 13. The figure demonstrates that the LCOE decreases as the inflation rate increases, demonstrating that the inflation rate plays a significant role in determining the LCOE.

Fig. 14 presents a sensitivity analysis of variations in capital cost, operating cost, and energy price on the IRR. The results indicate that if the capital cost decreases by 8% (green line), the IRR increases to 11.43%. According to the analysis, variations in operating cost have a relatively smaller effect on the IRR, primarily because of the high level of capital investment. As a result, the ratio of operating cost to capital cost, as well as the influence of energy price, is comparatively lower. However, operating cost has a significant influence on the calculation of the LCOE, leading to a larger gap between the LCOE and the energy selling price. Based on this analysis, if the energy price increases by 20%, the margin between the LCOE and the energy price widens, consequently increasing the IRR to ~12.5%. It is evident that if these variables change simultaneously, their combined effect on the IRR can also be evaluated.

4.3.2. *Geothermal plant's power production sensitivity*

Fig. 15 displays the variations in the geothermal plant's electrical power production and the system LCOE as the capacities of PV panels and wind turbines increases. In this figure, the numerical values (0.18–0.29 CAD$/kWh) correspond to the LCOE sensitivity surface, while the color represents geothermal power output. The electrical power output of the geothermal plant decreases with the increasing capacities of PV panels and wind turbines, and this reduction helps sustain the geo-reservoir's thermal energy capacity and long-term productivity.

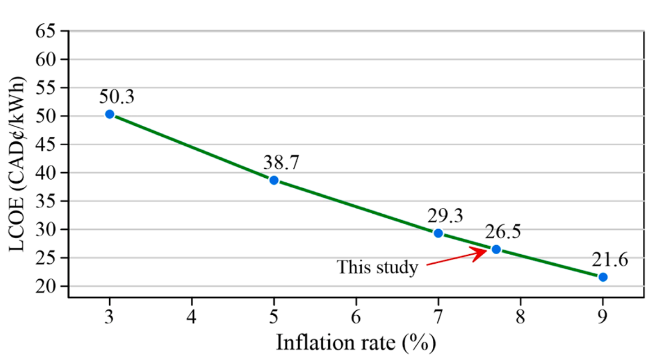

Fig. 13. Effect of inflation on the LCOE for the designed HDGP.

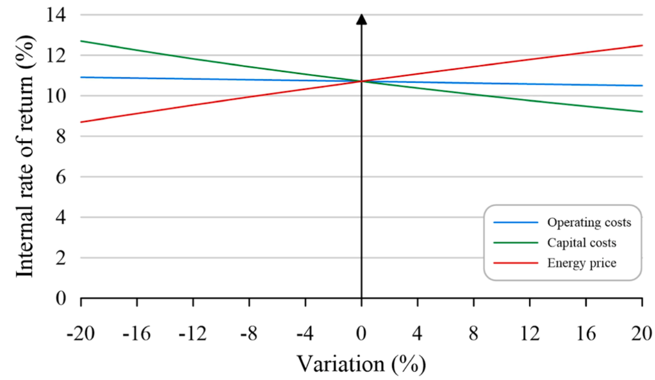

Fig. 14. Effect of variations in capital and operating costs, and energy price on the IRR of the designed HDGP.

4.3.3. *LCOE sensitivity*

The changes in the LCOE relative to an increase in the capacities of PV panels and wind turbines are shown in Fig. 16. The LCOE alters slightly with an increase in the capacity of the solar PV system. At the same time, this alteration is significantly greater with an increase in the capacity of the wind system. This difference is because of the wind system's higher investment and operating costs compared to the solar PV system.

4.3.4. *Energy price sensitivity*

Fig. 17 presents the sensitivity of the HDGP economic performance under different electricity price scenarios. The analysis demonstrates that the IRR of the HDGP increases significantly as the reference electricity price increases from the subsidized rate of ~0.30 CAD$/kWh to the unsubsidized rate of ~0.70 CAD$/kWh. Under the subsidized diesel scenario (~0.30 CAD$/kWh), the HDGP still achieves a positive IRR of 3.81%, confirming the economic feasibility of the system even under conservative market conditions. For the weighted average diesel tariff scenario (~0.50 CAD$/kWh), the IRR increases to 7.78%, while the unsubsidized diesel price scenario results in the highest IRR of 10.71%. These results confirm that the proposed HDGP remains economically competitive without considering government subsidies, grants, carbon credits, or renewable energy incentives in the LCOE calculation.

5. Conclusions and proposed future research

A techno-energy-economic feasibility evaluation was performed on an HDGP designed specifically for FL's Indigenous, off-grid, and fossil fuel-dependent community in CNT. This community is considered representative of similar communities in cold environments worldwide with suitable geothermal conditions. The evaluation was based on actual data/costs/prices for different HDGP components, chosen from a range of commercially available options. According to HOMER™'s optimization program, which aims to achieve the lowest LCOE, the hybridization strategy involved using the optimal capacities of wind turbines and PV panels to provide ~50% of FL's annual electrical power demand. This approach helps preserve the geo-reservoir's thermal energy efficiency and ensures stable productivity during the hybrid plant's operating life. The primary findings of this feasibility assessment are summarized as follows:

- The designed HDGP can deliver dispatchable and stable baseload electrical power to fulfill FL's yearly energy requirements over a 30-year lifespan, with an insignificant environmental footprint. The contributions of each electrical power producer in the HDGP were around 54% for the geothermal system, 25% for wind turbines, and 21% for PV panels.

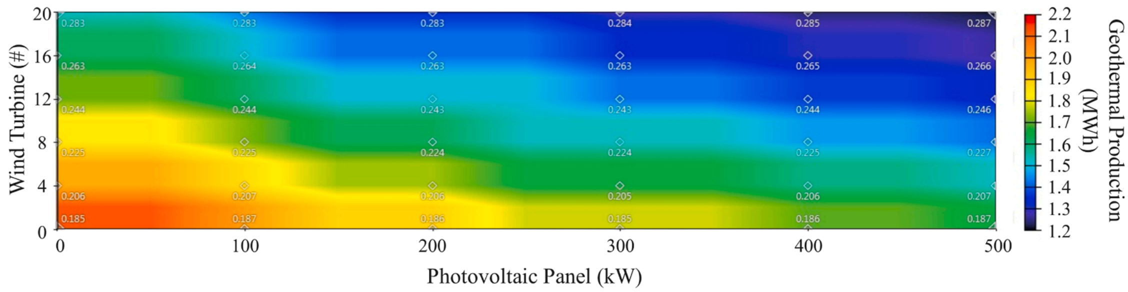

Fig. 15. Effect of PV panels and wind turbines on the geothermal plant's electrical power production.

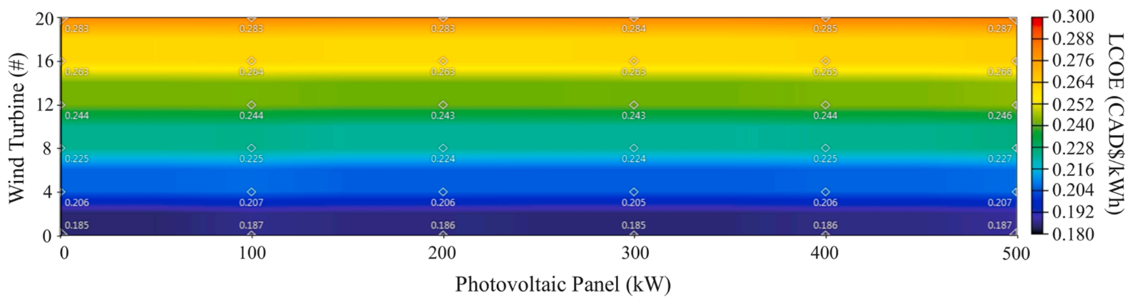

Fig. 16. Effect of PV panels and wind turbines on the LCOE.

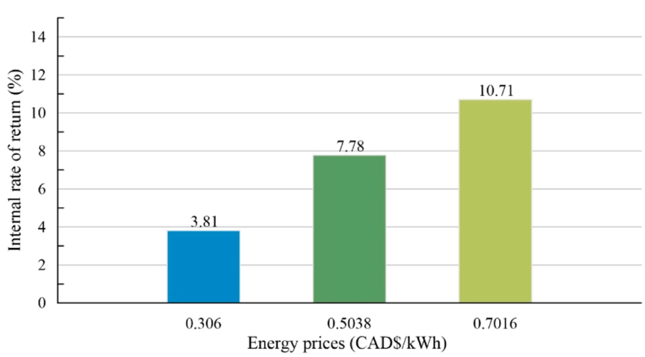

Fig. 17. Sensitivity analysis of the IRR of the designed HDGP under different subsidized and unsubsidized diesel electricity price scenarios.

- The HDGP generated ~2350 MWh of electricity per annum, which was slightly greater than FL's annual electricity consumption (~2147 MWh), and this excess can be used for the community's development.
- The BSS contributed substantially to supplying stable, reliable, and secure electrical energy for the community's demand, enabling independent operation for about three hours.
- The hybridization of wind, solar PV, and BSSs with the geothermal plant reduced the geothermal system's operating hours over the year, generally leading to an increase in the geothermal plant's operational lifecycle from 30 to ~43 years by allowing sufficient time for the geo-reservoir to recover its thermal energy capacity.
- The LCOE for the designed HDGP was calculated to be ~0.27 CAD $/kWh, whereas the LCOE for FL's current diesel-reliant facility, excluding government subsidies, was ~0.70 CAD$/kWh. This highlights the cost-effectiveness of the HDGP compared to the existing power generation system.
- The economic assessment showed an IRR of ~10.7% for the designed HDGP, which was slightly less than that of a stand-alone geothermal system (14.1%). Additionally, the PD for the HDGP was found to be ~13 years. This was slightly longer than that of a stand-alone geothermal plant (~11 years).
- The sensitivity analysis results indicated that increasing the capacity and number of wind turbines significantly affects the LCOE due to the high operational costs associated with wind systems. Consequently, the reduction in the margin between the LCOE and the energy price leads to a decrease in the IRR.
- Technical sensitivity analysis showed that increasing the capacity of wind turbines and PV panels significantly influenced the performance of the geothermal system. The results suggest that wind and solar systems can contribute to reducing the thermal load and enhancing geo-reservoir recovery.

The findings of this research can apply to similar societies in cold regions with favourable geothermal potential, supporting efforts to achieve decarbonization, as well as clean energy access and security goals.

This research outcomes align with several SDGs established by the United Nations in 2015. The HDGP directly advances SDG #7 (Affordable and Clean Energy) by delivering dispatchable, renewable baseload electricity at a cost 61% lower than the unsubsidized diesel alternative. The elimination of diesel consumption during normal operation supports SDG #13 (Climate Action) by removing the community's primary source of greenhouse gas emissions (~1450 tonnes CO_2eq/year avoided). Improved energy security and the reduced cost burden for Indigenous residents contribute to SDG #11 (Sustainable Cities and Communities), while the transferable methodology supports SDG #17 (Partnerships for the Goals) by providing a replicable framework for similar remote communities in cold-climate jurisdictions worldwide.

Future studies are proposed as follows:

- Conduct thermal, hydraulic, mechanical, and chemical simulations of the Nahanni/Manetoe Formations, which serves as the target geo-reservoir for geo-fluid extraction, over the project's lifespan.
- Perform systematic life cycle and socio-environmental assessments of the designed HDGP.
- Design and analyze the production and injection wells to prevent short-circuiting.
- Develop a smart system to properly monitor, control, and manage the hybrid system.

- Model and evaluate deep boreholes as energy storage systems for the proposed HDGP.
- Determine and address the practical implementation challenges faced by remote communities, particularly those located in cold environments, such as policy barriers, financing mechanisms, and maintenance logistics.

CRediT authorship contribution statement

Alireza Dehghani-Sanij: Writing – review & editing, Writing – original draft, Visualization, Validation, Software, Resources, Methodology, Investigation, Formal analysis, Data curation, Conceptualization. **Mohammad Hadi Ghasemi:** Writing – review & editing, Visualization, Software, Methodology, Investigation, Conceptualization. **Andrew Wigston:** Writing – review & editing, Visualization, Validation, Supervision, Resources, Investigation, Data curation, Conceptualization. **Kushsairy Kadir:** Writing – review & editing, Validation, Supervision, Resources, Investigation, Conceptualization. **Maurice B. Dusseault:** Writing – review & editing, Visualization, Validation, Supervision, Resources, Investigation, Conceptualization. **Grant D. Wach:** Conceptualization, Methodology, Resources, Supervision, Validation, Visualization, Writing – review & editing.

Declaration of competing interest

The authors declare that they have no known competing financial interests or personal relationships that could have appeared to influence the work reported in this paper.

Acknowledgements

The authors sincerely appreciate the support of the UniKL British Malaysian Institute and the Institute of Postgraduate Studies, Universiti Kuala Lumpur, through the UniKL Excellent Research Grant Scheme (UERGS), UniKL/CoRI/UER22003.

Data availability

The data used and analyzed during this research are confidential but available from the corresponding author upon request.

References

[1] A.R. Dehghani-Sanij, M.N Bahadori, *Ice-houses: Energy, architecture, and sustaina*bility. 1st ed, Elsevier, Imprint by Academic Press, 2021, https://doi.org/10.1016/C2019-0-04261-6.
[2] M.M. Rahman, Z. Khan, S. Khan, et al., Disaggregated energy consumption, industrialization, total population, and ecological footprint nexus: evidence from the world's top 10 most populous countries, Env. Sci. Pollut. Res. 30 (2023) 119069–119083, https://doi.org/10.1007/s11356-023-30499-4.
[3] S. Gao, J. Jiang, S. Zhu, B. Aslam, W. Wang, Nonlinear influence of per capita carbon emissions, newborn birth rate, renewable energy, industrialization, and economic growth on urbanization: new evidence from panel threshold model, Energy Strat. Rev. 51 (2024) 101305, https://doi.org/10.1016/j.esr.2024.101305.
[4] M.M. Rahman, M. Husnain, M.N. Azimi, An environmental perspective of energy consumption, overpopulation, and human capital barriers in South Asia, Sci. Rep. 14 (2024) 4420, https://doi.org/10.1038/s41598-024-53950-z.
[5] Q. Hassan, P. Viktor, T.J. Al-Musawi, B.M. Ali, S. Algburi, et al., The renewable energy role in the global energy transformations, Renew. Energy Focus 48 (2024) 100545, https://doi.org/10.1016/j.ref.2024.100545.
[6] Energy Institute, Statistical review of world energy 2024: electricity and renewables. 73rd edition. https://www.energyinst.org/statistical-review, 2024 (Accessed 17 March 2026).
[7] A.R. Dehghani-Sanij, A. Wigston, T. Takeda, A. Al-Haq, M.B. Dusseault, R.A. Fraser, *Feasibility assessment of using a geothermal system in Canada's remote Northern* communities (Fort Liard, Northwest Territories), in: Second EAGE Workshop on Geothermal Energy in Latin America, Guanacaste, Costa Rica, Nov, 2023, pp. 15–17, https://doi.org/10.3997/2214-4609.202385005.
[8] A.R. Dehghani-Sanij, A. Wigston, M. Razavi, M.B. Dusseault, R.A. Fraser, Feasibility evaluation of a hybrid, deep geothermal plant in remote Northern areas of Canada, in: First EAGE Symposium and Exhibition on Geosciences for New Energies in America, Mexico City, Mexico 2024, 2024, pp. 1–6, https://doi.org/10.3997/2214-4609.202487001. Dec. 3–5.
[9] A.R. Dehghani-Sanij, M.B. Dusseault, S.A. Smart, Hybrid, integrated, and engineered geothermal (SHIEG) systems, npj Therm. Sci. Eng. 1 (2026) 9, https://doi.org/10.1038/s44435-026-00009-2.
[10] M.M. Miranda, F.-A. Comeau, J. Raymond, L. Gosselin, et al., Geothermal resources for energy transition: a review of research undertaken for remote northern Canadian communities, Eur. Geol. 54 (2022) 12–20, https://doi.org/10.5281/zenodo.7882811.
[11] S.B. Mahbaz, A.R. Dehghani-Sanij, M.B. Dusseault, J.S. Nathwani, Enhanced, integrated geothermal system for sustainable development of Canada's Northern communities, Sustain. Energy Technol. Assess. 37 (2020) 100565, https://doi.org/10.1016/j.seta.2019.100565.
[12] ThinkGeoEnergy. ThinkGeoEnergy's, Top 10 geothermal countries 2024 – power. https://www.thinkgeoenergy.com/thinkgeoenergys-top-10-geothermal-countries-2024-power/#:~:text=The%20global%20geothermal%20power%20generation,promise%20further%20expansion%20in%202025, 2026 (Accessed 17 March 2026).
[13] B.A. Goldstein, G. Hiriart, J. Tester, B. Bertani, R. Bromley, L. Gutierrez-Negrin, E. Huenges, A. Ragnarsson, A. Mongillo, H. Muraoka, V.I. Zui, Great expectations for geothermal energy to 2100, in: Proceedings 36th Workshop on Geothermal Reservoir Engineering, Vol. 665, SGP-TR-191, Stanford, CA, USA, Feb. 2, 2011. Jan. 31 –.
[14] S.B. Mahbaz, A. Yaghoubi, A.R. Dehghani-Sanij, E. Sarvaramini, Y. Leonenko, M. B. Dusseault, Well-doublets: a first-order assessment of geothermal SedHeat systems, Appl. Sci. 11 (2) (2021) 697, https://doi.org/10.3390/app11020697.
[15] C. Kinney, A.R. Dehghani-Sanij, S.B. Mahbaz, M.B. Dusseault, J.S. Nathwani, R. A. Fraser, Geothermal energy for sustainable food production in Canada's remote northern communities, Energies 12 (21) (2019) 4058, https://doi.org/10.3390/en12214058.
[16] A.R. Dehghani-Sanij, Feasibility assessment of hybrid geothermal systems in remote northern Canadian communities, Report prepared for CanmetENERGY-Ottawa, NRCan, Ottawa, ON, Canada, 2023.
[17] T.F. Agajie, A. Fopah-Lele, I. Amoussou, et al., Enhancing Ethiopian power distribution with novel hybrid renewable energy systems for sustainable reliability and cost efficiency, Sci. Rep. 14 (2024) 10711, https://doi.org/10.1038/s41598-024-61413-8.
[18] H. Khurshid, B.S. Mohammed, A.M. Al-Yacoubya, M.S. Liew, N.A. Zawawi, Analysis of hybrid offshore renewable energy sources for power generation: a literature review of hybrid solar, wind, and waves energy systems, Dev. Built Environ. 19 (2024) 100497, https://doi.org/10.1016/j.dibe.2024.100497.
[19] A.A. Alhijazi, R.A. Almasri, A.F. Alloush, A hybrid renewable energy (Solar/Wind/Biomass) and multi-use system principles, types, and applications: a review, Sustainability 15 (24) (2023) 16803, https://doi.org/10.3390/su152416803.
[20] D.A. Pérez Uc, S.E. de León Aldaco, Aguayo Alquicira J. trends in hybrid renewable energy system (HRES) applications: a review, Energies 17 (11) (2024) 2578, https://doi.org/10.3390/en17112578.
[21] S. Yadav, P. Kumar, A. Kumar, Optimal design and energy management in isolated renewable sources based microgrid considering excess energy and reliability aspects, J. Energy Storage 103 (2024) 114320, https://doi.org/10.1016/j.est.2024.114320.
[22] S. Yadav, P. Kumar, A. Kumar, Excess energy management and techno-economic analysis of optimal designed isolated microgrid with reliability and environmental aspects, Energy Convers. Manag. 333 (2025) 119772, https://doi.org/10.1016/j.enconman.2025.119772.
[23] S. Yadav, P. Kumar, A. Kumar, Energy management and techno-economic-environmental analysis of hybrid renewable energy based isolated microgrid with various energy storage technologies, Int. J. Hydrog. Energy 217 (2026) 153890, https://doi.org/10.1016/j.ijhydene.2026.153890.
[24] A. Masih, H.K. Verma, Optimum sizing and simulation of hybrid renewable energy system for remote area, Energy Environ. 33 (5) (2022) 933–951, https://doi.org/10.1177/0958305X21103011.
[25] W. He, L. Tao, L. Han, Y. Sun, P.E. Campana, J. Yan, Optimal analysis of a hybrid renewable power system for a remote island, Renew. Energy 179 (2021) 96–104, https://doi.org/10.1016/j.renene.2021.07.034.
[26] M.H. Shahverdian, A. Sohani, H. Sayyaadi, A 3E water energy nexus based optimum design for a hybrid PV-PEMFC electricity production systems for off-gird applications, Energy Convers. Manag. 267 (2022) 115911, https://doi.org/10.1016/j.enconman.2022.115911.
[27] M.H. Shahverdian, S. Sedayevatan, M. Hosseini, Multi-objective technoeconomic optimization of an off-grid solar-ground-source driven cycle with hydrogen storage for power and fresh water production, Int. J. Hydrog. Energy 48 (52) (2023) 19772–19791, https://doi.org/10.1016/j.ijhydene.2023.02.062.
[28] S.A. Behmounesi, A. Saraei, H. Afshar, H.A. Ashtiani, A.R. Dehghani-Sanij, Techno-economic analysis of optimally hybrid photovoltaic-wind systems to meet the energy demand of a residential building in six different areas of Iran, Energy Convers. Manag. 322 (2024) 119131, https://doi.org/10.1016/j.enconman.2024.119131.
[29] S. Basnet, K. Deschinkel, L. Le Moyne, M.C Péra, A review on recent standalone and grid integrated hybrid renewable energy systems: system optimization and energy management strategies, Renew. Energy Focus 46 (2023) 103–125, https://doi.org/10.1016/j.ref.2023.06.001.
[30] J. Jurasz, M. Guezgouz, P.E. Campana, A. Kies, On the impact of load profile data on the optimization results of off-grid energy systems, Renew. Sustain. Energy Rev. 159 (2022) 112199, https://doi.org/10.1016/j.rser.2022.112199.
[31] I. Ahmed, M.A. Razzak, F. Ahmed, Sustainable hybrid renewable energy management system for a community in island: a model approach utilising hybrid optimization of multiple energy resources optimization and priority setting-based

supervisory control and data acquisition operation, IET Smart Grid. 7 (2024) 940–966, https://doi.org/10.1049/stg2.12192.
[32] T. Falope, L. Lao, D. Hanak, D. Huo, Hybrid energy system integration and management for solar energy: a review, Energy Convers. Manag.: X 21 (2024) 100527, https://doi.org/10.1016/j.ecmx.2024.100527.
[33] W. Wang, D. Simonson, Techno-economic assessment of PV-diesel-battery hybrid systems for poultry farms: a case study in North Carolina, Energy Nexus. 17 (2025) 100372, https://doi.org/10.1016/j.nexus.2025.100372.
[34] M. Mahmoud, S. Haridy, A. Mdallal, et al., Modelling and optimization of a hybrid photovoltaic-parabolic trough concentrated solar power plant: technical, economic, and environmental, Energy Nexus. 18 (2025) 100436, https://doi.org/10.1016/j.nexus.2025.100436.
[35] H. Hajabdollahi, M.A. Pour, M. Shafiey Dehaj, Cogeneration system utilizing geothermal energy: energy, exergy, economic and environmental analyses and multi-objective optimization, Energy Nexus. 21 (2026) 100642, https://doi.org/10.1016/j.nexus.2026.100642.
[36] S. Salari, A. Etminan, M. Jamil, Design and performance evaluation of a hybrid renewable energy system integrating wind, diesel generators, and battery storage for remote communities, Energies 19 (7) (2026) 1676, https://doi.org/10.3390/en19071676.
[37] A.G. Olabi, M. Mahmoud, B. Soudan, T. Wilberforce, M. Ramadan, Geothermal based hybrid energy systems, toward eco-friendly energy approaches, Renew. Energy 147 (1) (2020) 2003–2012, https://doi.org/10.1016/j.renene.2019.09.140.
[38] B.W. Kariuki, H. Hassan, M. Ahmed, M. Emam, A review on geothermal-solar hybrid systems for power production and multi-generation systems, Appl. Therm. Eng. 259 (2025) 124796, https://doi.org/10.1016/j.applthermaleng.2024.124796.
[39] B. Bokelman, E.E. Michaelides, D.N. Michaelides, A geothermal-solar hybrid power plant with thermal energy storage, Energies 13 (5) (2020) 1018, https://doi.org/10.3390/en13051018.
[40] C. Zhou, E. Doroodchi, B. Moghtaderi, An in-depth assessment of hybrid solar–geothermal power generation, Energy Convers. Manag. 74 (2013) 88–101, https://doi.org/10.1016/j.enconman.2013.05.014.
[41] H.I. Fedakar, A.E. Dinçer, A. Demir, Comparative analysis of hybrid geothermal-solar systems and solar PV with battery storage: site suitability, emissions, and economic performance, Geothermics 125 (2025) 103175, https://doi.org/10.1016/j.geothermics.2024.103175.
[42] T. Hai, J. Zhou, Y.S. Almashhadani, R. Chaturvedi, A.H. Alshahri, H.R. Almujibah, A.S. Metwally, M. Ullah, Thermo-economic and environmental assessment of a combined cycle fueled by MSW and geothermal hybrid energies, Process Saf. Environ. Prot. 176 (2023) 260–270, https://doi.org/10.1016/j.psep.2023.05.067.
[43] M. Tafavogh, A. Zahedi, Design and production of a novel encapsulated nano phase change materials to improve thermal efficiency of a quintuple renewable geothermal/hydro/biomass/solar/wind hybrid system, Renew. Energy 169 (2021) 358–378, https://doi.org/10.1016/j.renene.2020.12.118.
[44] A. Bozkurt, M.S. Genç, Optimization of energy and hydrogen storage systems in geothermal energy sourced hybrid renewable energy system, Process Saf. Environ. Prot. 189 (2024) 1052–1060, https://doi.org/10.1016/j.psep.2024.06.128.
[45] M.R. Naseh, E. Behdani, Feasibility study for size optimisation of a geothermal/PV/wind/diesel hybrid power plant using the harmony search algorithm, Int. J. Sustain. Energy 40 (6) (2021) 584–601, https://doi.org/10.1080/14786451.2020.1835907.
[46] O. Bamisile, C. Dongsheng, J. Li, M. Mukhtar, X. Wang, J. Duo, R. Cao, Q. Huang, An innovative approach for geothermal-wind hybrid comprehensive energy system and hydrogen production modeling/process analysis, Int. J. Hydrog. Energy 47 (27) (2022) 13261–13288, https://doi.org/10.1016/j.ijhydene.2022.02.084.
[47] S. Asal, A. Acir, I. Dincer, Comparative assessment of chloride family hydrogen production cycles driven by a nuclear-geothermal energy system, Comput. Chem. Eng. 194 (2025) 108967, https://doi.org/10.1016/j.compchemeng.2024.108967.
[48] J. Liu, C.Y. Hsu, S.F. Ahmad, M.A. Alotaibi, M.I. Allahham, M. Qin, Design and energy, exergy, thermoeconomic, and exergo-environmental (4E) analyses of a novel hybrid geothermal/biogas-powered green multi-generation system using a post-combustion CO_2 capture unit, Appl. Energy 377 (2025) 124662, https://doi.org/10.1016/j.apenergy.2024.124662.
[49] S. Yadav, P. Kumar, A. Kumar, Techno-economic assessment of hybrid renewable energy system with multi energy storage system using HOMER, Energy 297 (2024) 131231, https://doi.org/10.1016/j.energy.2024.131231.
[50] S. Yadav, P. Kumar, A. Kumar, Hybrid renewable energy systems design and techno-economic analysis for isolated rural microgrid using HOMER, Energy 327 (2025) 136442, https://doi.org/10.1016/j.energy.2025.136442.
[51] S. Yadav, P. Kumar, A. Kumar, Energy management and techno-economic-environmental analysis of hybrid renewable energy based isolated microgrid with various energy storage technologies, Int. J. Hydrog. Energy 217 (2026) 153890, https://doi.org/10.1016/j.ijhydene.2026.153890.
[52] M.F.H. Mojumder, T. Islam, M.M.R. Rafi, et al., Enhanced hybrid energy generation solutions for sustainable rural electrifications in Bangladesh: a system optimization and performance evaluation approach using HOMER Pro and MATLAB/Simulink, J. Energy Storage 115 (2025) 115971, https://doi.org/10.1016/j.est.2025.115971.
[53] M.F.H. Mojumder, T. Islam, P. Chowdhury, et al., Techno-economic evaluation of various hybrid energy systems optimization for rural Bangladesh, in: 2024 IEEE International Conference on Power, Electrical, Electronics and Industrial Applications (PEEIACON), Rajshahi, Bangladesh, 2024, https://doi.org/10.1109/PEEIACON63629.2024.10800667. Sep. 12–13.
[54] M.F.H. Mojumder, T. Islam, N.A. Takia, et al., Enhancing energy economics using hybrid renewable energy systems on the permanent campus of Dhaka international university, in: 2024 3rd International Conference on Advancement in Electrical and Electronic Engineering (ICAEEE), Gazipur, Bangladesh, 2024, pp. 25–27, https://doi.org/10.1109/ICAEEE62219.2024.10561680. Apr.
[55] P. Dey, H. Baidya, M.T.R. Zisan, et al., Design optimization and techno-economic analysis of off-grid hybrid energy systems for sustainable rural electrification in Bangladesh, in: 2024 IEEE International Women in Engineering (WIE) Conference on Electrical and Computer Engineering (WIECON-ECE), Chennai, India, 2024, pp. 6–7, https://doi.org/10.1109/WIECON-ECE64149.2024.10915104, 06-07 Dec.
[56] M. Hasan, N.A. Zarin, M.R. Ahmed, O. Farrok, Global pathways for hybrid renewable energy systems: challenges, solutions, policy, and regulatory frameworks, Energy Convers. Manag.: X 29 (2026) 101534, https://doi.org/10.1016/j.ecmx.2026.101534.
[57] K. Talukder, N.A. Zarin, N.R. Nobonita, et al., Towards sustainable lithium-ion battery recycling in Bangladesh: assessing environmental aspects and future prospects, Energy Nexus. 22 (2026) 100698, https://doi.org/10.1016/j.nexus.2026.100698.
[58] R.Q. Momani, A. Abuelrub, H.M.K. Al-Masri, A.Q. Al-Shetwi, Cost-optimal sizing of battery energy storage systems in microgrids using artificial rabbits optimization, Energy Nexus. 19 (2025) 100486, https://doi.org/10.1016/j.nexus.2025.100486.
[59] R. Alsaqqar, A. Abuelrub, Optimization of hybrid renewable energy systems: reliability, cost, and environmental trade-offs using PSO and GJO algorithms, Clean. Eng. Technol. 30 (2026) 101131, https://doi.org/10.1016/j.clet.2025.101131.
[60] A.R. Dehghani-Sanij, Thermal efficiency study of geothermal power plants in Northern Canada, Report Prepared for CanmetENERGY-Ottawa, NRCan, Ottawa, ON, Canada, 2025.
[61] S. Abdollahiarpanahi, M. Jahangiri, S. Shahgholian, M. Taheri, Finding the best station in Canada for using residential scale solar heating: a multicriteria decision-making analysis, Int. Trans. Electr. Energy Syst. 2024 (1) (2024) 8843981, https://doi.org/10.1155/etep/8843981.
[62] K. Huang, A.R. Dehghani-Sanij, C. Hickson, S.E. Grasby, et al., Canada's geothermal energy update in 2023, Energies 17 (8) (2024) 1807, https://doi.org/10.3390/en17081807.
[63] J. Knowles, Power shift: electricity for Canada's remote communities, in: The Conference Board of Canada, Ottawa, ON, Canada, 2016. https://www.conferenceboard.ca/product/power-shift-electricity-for-canadas-remote-communities/ (Accessed 11 December 2024).
[64] D. Lovekin, D. Heerema, Diesel, renewables, and the Future of Canada's remote communities: Introduction to Microgrids, The Pembina Institute, Canada, 2019. https://www.pembina.org/blog/remote-microgrids-intro (Accessed 11 December 2024).
[65] Government of Canada, Pan-canadian framework on clean growth and climate change: Canada's plan to address climate change and grow the economy, Environment and Climate Change Canada, Gatineau, QC, Canada, 2016. https://publications.gc.ca/site/eng/9.828774/publication.html (Accessed 11 December 2024).
[66] J.-P Pinard, in: A. Trimble (Ed.), Fort liard wind site potential study, Report prepared for Aurora Research Institute, Aurora College, Inuvik, NT, Canada, March 2017. https://nwtresearch.com/sites/default/files/ftliard2017.pdf (Accessed 11 December 2024).
[67] Northwest Territories Power Corporation (NTPC), Here's how we supply power in your community, Hay River, NT, Canada, 2022 ntpc.com/your-community/community-map(Accessed 11 December 2024).
[68] Natural Resources Canada (NRCan), Community-based geothermal demonstration in remote first nations community, Rep. prep. Boreal. Geopower Inc, NRCan Can. (2018). https://www.nrcan.gc.ca/science-and-data/funding-partnerships/funding-opportunities/current-investments/community-based-geothermal-demonstration-remote-first-nations-community/12410 (Accessed 11 December 2024).
[69] Northwest Territories Power Corporation (NTPC), Generation in Fort Liard 2019-20, Hay River, NT, Canada, 2022.
[70] J. Majorowicz, S.E. Grasby, Deep geothermal heating potential for the communities of the Western Canadian sedimentary basin, Energies 14 (3) (2021) 706, https://doi.org/10.3390/en14030706.
[71] S.E. Grasby, J. Majorowicz, G. McCune, Geothermal energy potential for Northern communities. Open file 7350, Geological Survey of Canada, NRCan, Ottawa, ON, Canada, 2013.
[72] C. Dunn, Acho Dene Koe (ADK)/Borealis geothermal energy project: geological & geothermal energy resource assessment, Report prepared by Borealis GeoPower Inc.,, Canada, 2011.
[73] J. Majorowicz, S.E. Grasby, Geothermal energy for Northern Canada: is it economical? Nat. Resour. Res. 23 (2014) 159–173, https://doi.org/10.1007/s11053-013-9199-3.
[74] Lawless J., Seastres J., Malate C., Charroy J. Fort liard geothermal technical due diligence, integrated report. reviewed and approved by Sinclair Knight Merz (SKM) Ltd, Northwest Territories Hydro Corporation (NTHC), registry.mvlwb.ca/Documents/MV2012L4-0001/MV2012L4-0001%20-%20Borealis%20Geopower%20-%20Technical%20Session%20-%20IR1%20-%20SKM%20Report%20-%20Mar19-12.pdf; 2012 (Accessed 17 March 2026).
[75] S. Hu, Z. Yang, J. Li, Y. Duan, Optimal solar thermal retrofit for geothermal power systems considering the lifetime brine degradation, Renew. Energy 186 (2022) 628–645, https://doi.org/10.1016/j.renene.2022.01.028.
[76] M. Gehringer, V. Loksha, Geothermal handbook: planning and financing power generation. technical report 002/12, energy sector management assistance program, The World Bank Group, Washington, USA, 2012.
[77] Z. Novak Pintarič, Z. Kravanja, The importance of using discounted cash flow methodology in techno-economic analyses of energy and chemical production

plants, J. Sustain. Dev. Energy Water Environ. Syst. 5 (2) (2017) 163–176, https://doi.org/10.13044/j.sdewes.d5.0140.

[78] G. Drozdowski, P. Dziekański, Net present value as a reinforcement of the decision-making process in investment selection, Infrastructures 6 (2022) 66–67, https://doi.org/10.32843/infrastruct66-7.

[79] D.W. Morrow, K. Aulstead, Convection-driven subsurface hydrothermal dolomitization in Middle Devonian-age shallow water limestones in the 0.4 tcf Kotaneelee gas field of southeastern Yukon territory, in: Dolomites—The Spectrum: Mechanisms, Models, Reservoir Development—Seminar and Core Conference, Canadian Society of Petroleum Geologists, Calgary, AB, Canada, 2004, pp. 13–15. Jan.

[80] Y.A. Cengel, M.A. Boles, M. Kanoğlu, *Thermodynamics: an engineering approach*. 10th ed, McGraw Hill, New York, NY, 2024.

[81] M. Lips, Length of operational life and its impact on life-cycle costs of a tractor in Switzerland, Agriculture 7 (8) (2017) 68, https://doi.org/10.3390/agriculture7080068.

[82] HOMER™ Energy, HOMER pro version 3.15 [software]. real discount rate. https://homerenergy.com/products/pro/docs/latest/real_discount_rate.html, 2026 (Accessed 17 March 2026).

[83] HOMER™ Energy, HOMER pro version 3.15 [software]. capital recovery factor. https://homerenergy.com/products/pro/docs/latest/capital_recovery_factor.html, 2026 (Accessed 17 March 2026).

[84] HOMER™ Energy, HOMER pro version 3.15 [software]. levelized cost of energy. https://www.homerenergy.com/products/pro/docs/3.15/levelized_cost_of_energy.html, 2026 (Accessed 17 March 2026).

[85] S. Hoseinzadeh, F. Pourfayaz, Feasibility assessment of a 10-MW grid-connected photovoltaic power plant for small industries: a case study in Iran, J. Therm. Anal. Calorim. 149 (24) (2024) 14901–14912, https://doi.org/10.1007/s10973-024-13716-1.

[86] J. Huang, J. Tong, P. Wang, X. Zheng, Application and comparison of NPV and IRR methods in company investment decisions, in: Proc 7th Int Conf Financial Innovation and Economic Development (ICFIED 2022), Zhuhai, China, 2022, https://doi.org/10.2991/aebmr.k.220307.012.

[87] L. Sukamdani, G. Apriyanto, M. Burhan, Investment feasibility in the framework of implementation cooperation in the utilization of regional property, Int. J. Finance Bank. Stud. 12 (2023) 13–23, https://doi.org/10.20525/ijfbs.v12i3.2866.

[88] HOMER™ Energy, HOMER pro version 3.15 [software]. salvage value. https://www.homerenergy.com/products/pro/docs/3.15/salvage_value.html, 2026 (Accessed 17 March 2026).

[89] Government of Canada, Environment and climate change Canada, Emiss. Factors Ref. Values: Can. Greenh. Gas Offset Credit Syst. (2025). Version 3.0. https://publications.gc.ca/collections/collection_2025/eccc/En84-294-2025-eng.pdf. Oct (Accessed 27 May 2026)

[90] G. Axelsson, V. Stefánsson, G. Björnsson, S. Liu, Sustainable geothermal utilization – case histories; definitions; research issues and modelling, Geothermics 39 (4) (2010) 283–291, https://doi.org/10.1016/j.geothermics.2010.08.001.

[91] F.V. Hackstein, R. Madlener, Sustainable operation of geothermal power plants: why economics matters, Geotherm. Energy 9 (10) (2021), https://doi.org/10.1186/s40517-021-00183-2.